Berry Phase, Berry Connection, and Chern Number for a Continuum Bianisotropic Material From a Classical Electromagnetics Perspective

S. Ali Hassani Gangaraj, *Graduate Student Member, IEEE*, Mário G. Silveirinha, *Fellow, IEEE*, and George W. Hanson, *Fellow, IEEE*

***Abstract*—The properties that quantify photonic topological insulators (PTIs), Berry phase, Berry connection, and Chern number, are typically obtained by making analogies between classical Maxwell's equations and the quantum mechanical Schrödinger equation, writing both in Hamiltonian form. However, the aforementioned quantities are not necessarily quantum in nature, and for photonic systems they can be explained using only classical concepts. Here, we provide a derivation and description of PTI quantities using classical Maxwell's equations, demonstrate how an electromagnetic mode can acquire Berry phase, and discuss the ramifications of this effect. We consider several examples, including wave propagation in a biased plasma, and radiation by a rotating isotropic emitter. These concepts are discussed without invoking quantum mechanics and can be easily understood from an engineering electromagnetics perspective.**

***Index Terms*—Berry phase, photonic topological insulator (PTI), surface wave.**

I. Introduction

PHOTONIC topological insulators (PTIs) are emerging as an important class of material (natural or meta) that allows for the propagation of unidirectional surface waves, immune to backscattering, at the interface with another medium [1]–[5]. There are different types of photonic topological materials; but, in this paper, we focus on the simplest subclass formed by media with broken time reversal (TR) symmetry, sometimes also designated as Chern-type insulators (the analogs of quantum Hall insulators). The properties of these materials are quantified by the Berry phase, Berry connection, and an invariant known as the Chern number [6]–[9]. Berry phase was first proposed in 1984 [10] for quantum systems undergoing cyclic evolution. While the occurrence of a phase factor as a quantum system evolved was long known in quantum mechanics, it was thought to be nonobservable since a gauge transformation could remove it. It was Berry who showed that for a cyclic variation, and assuming adiabatic (sufficiently slow) evolution, the phase is not removable under a gauge transformation [10], and is also observable. It is a form of geometric phase related to parallel transport of a vector along a curved surface.[1] The concept has been generalized for nonadiabatic evolution [11]. In quantum mechanics, a prototypical example is the progression of electron spin as a magnetic field vector rotates in a cyclical manner [12], [13]. Here, we are interested in electromagnetic propagation and the Berry phase that a classical electromagnetic wave acquires as it propagates (wave propagation being a form of cyclic evolution, e.g., the field polarization returning to its initial position after every wavelength of propagation). See [14]–[18] for some reviews of optical phenomena related to Berry phase. Although not discussed here, we mention another effect related to the Berry phase, the spin Hall effect of light, which is a geometric Berry-phase counterpart of the Lorentz force. This effect has been extensively studied and experimentally verified [19]–[21].

Often, Berry properties are obtained using the quantum mechanical derivation based on a Hamiltonian and making an analogy between Maxwell's equations and the quantum system. However, this approach has two drawbacks: it necessitates knowledge of quantum mechanics, and, more importantly, it obscures the true nature of the phenomena, which in this case is classical.

There have been previous works considering Berry quantities for electromagnetics from a classical perspective [15]–[25], which is intimately connected with spin-orbit interactions in light [26], and from a relativistic wave-equation perspective in [27], [28]. However, many previous classical works invoke the theory of Hermitian line bundles or gauge theory (see, e.g., [16], [22]), and, here, we avoid those topics and consider Berry properties from a relatively simple electromagnetic perspective [29]. Furthermore, as described in [30], before the Berry phase was understood as the general concept it is now, in various fields this extra phase had been found. In electromagnetics, the most notable discoveries were by Pancharatnam in 1956 [31], who studied polarization evolution of light, and Budden and Smith [32], [33], who considered propagation through the ionosphere, modeled as an inhomogeneous medium whose parameters varied gradually with height. Further, pioneering works were done

Manuscript received November 5, 2016; revised December 14, 2016; accepted January 11, 2017. Date of current version February 24, 2017.

S. A. Hassani Gangaraj and G. W. Hanson are with the Department of Electrical Engineering, University of Wisconsin–Milwaukee, Milwaukee, WI 53211 USA (e-mail: ali.gangaraj@gmail.com.edu; george@uwm.edu).

M. G. Silveirinha is with the Instituto Superior Técnico, University of Lisbon and Instituto de Telecomunicações, Torre Norte, Lisbon 1049-001, Portugal (e-mail: mario.silveirinha@co.it.pt).

Color versions of one or more of the figures in this paper are available online at http://ieeexplore.ieee.org.

Digital Object Identifier 10.1109/JMMCT.2017.2654962

[1] "One widely used example is moving a swinging pendulum from one point on a sphere, along some contour, and back to the original point-the geometric phase is given by the solid angle subtended by the path of movement." See [12].

by Rytov in 1938, [34], and Vladimirskii in 1941, [35], describing geometrical properties of the polarization evolution of light along curvilinear trajectories; the spin-redirection geometric phase in optics discussed here is sometimes called the *Rytov–Vladimirskii–Berry* phase. The topic of parallel transport of the polarization of light in an inhomogeneous medium was discussed as early as 1926 by Bortolotti [36].

Thus, we can categorize the geometric phases in optics into two classes: 1) The spin-redirection/Rytov–Vladimirskii–Berry) geometric phase, which is the phase associated with changes in wave momentum (with a conserved polarization state), and is the subject of this paper and 2) the Pancharatnam–Berry phase, which appears when the polarization state varies on the Poincare sphere (while the momentum is unchanged). Here, we consider electromagnetic propagation through a uniform, homogeneous medium, in order to consider perhaps the simplest possible example where important Berry effects occur.

After the discovery of the Berry phase, an early example of a photonic systems exhibiting such an effect was given in [37], [38], which considered the rotation of the polarization vector of a linearly polarized laser beam traveling through a single, helically wound optical fiber. More recently, and of more direct interest here, there has been a lot of work on various photonic systems that demonstrate nontrivial Berry properties, both for periodic and continuum materials [39]–[41]. The principal interest in these systems is because at the interface between two regions with different Berry curvatures, a backscattering-immune (i.e., unidirectional) surface plasmon polariton (SPP) can propagate. If the operational frequency is in a common bandgap of the two bulk materials, the SPP is also immune to diffraction, and so even arbitrarily large discontinuities do not scatter energy.

We also note that one-way SPPs at, e.g., biased plasma interfaces, have been observed long before the Berry phase concept [42], [43], and later, although not within the framework of Berry properties [44]. One-way SPPs can also be formed at various other interfaces, such as at the domain walls of Weyl semimetals with broken TR symmetry [45].

One approach to create PTIs is to use two-dimensional (2-D) photonic crystals with degenerate Dirac cones in their band structure [6], [7]. The degeneracy can be lifted by breaking TR symmetry, which opens a band gap and leads to topologically nontrivial photonic bands. Continuum materials, either homogenized metamaterials or natural materials, supporting topologically-protected unidirectional photonic surface states have also recently been shown [41]–[47]. Unidirectional surface modes at the interface between a magnetized plasma or magnetized ferrite and a metal have been recently studied [48]–[50], where TR symmetry is broken by applying a static magnetic field, opening a bandgap and inducing nontrivial Berry properties.

Unidirectional, scattering-immune surface-wave propagation has great potential for various waveguiding device applications. The aim of this paper is to derive and explain all Berry properties from a classical engineering electromagnetic perspective, without consideration of the usual quantum mechanics derivation, appealing to analogies between Schrödinger's equations and Maxwell's equations, or invoking gauge theories.

II. Theory

A. Maxwell's Equations as a Momentum-Dependent Eigenvalue Problem

In order to establish the necessary concepts, we start by considering a dispersionless material model, but later extend the results to a lossless dispersive material model.

Source-free Maxwell's equations are

$$\nabla \times \mathbf{E}(\mathbf{r},t) = -\frac{\partial}{\partial t}\mathbf{B}(\mathbf{r},t),$$
$$\nabla \times \mathbf{H}(\mathbf{r},t) = \frac{\partial}{\partial t}\mathbf{D}(\mathbf{r},t), \tag{1}$$

and working in the momentum–frequency domain ($\partial/\partial t \to -i\omega$ and $\nabla \to i\mathbf{k}$) and considering a homogeneous, lossless, bianisotropic material with frequency-independent dimensionless parameters $\boldsymbol{\varepsilon}$, $\boldsymbol{\mu}$, $\boldsymbol{\xi}$, $\boldsymbol{\varsigma}$ representing permittivity, permeability, and magnetoelectric coupling tensors, respectively, the constitutive relations are

$$\begin{pmatrix}\mathbf{D}(\mathbf{k},\omega)\\ \mathbf{B}(\mathbf{k},\omega)\end{pmatrix} = \begin{pmatrix}\varepsilon_0\boldsymbol{\varepsilon} & \frac{1}{c}\boldsymbol{\xi}\\ \frac{1}{c}\boldsymbol{\varsigma} & \mu_0\boldsymbol{\mu}\end{pmatrix}\cdot\begin{pmatrix}\mathbf{E}(\mathbf{k},\omega)\\ \mathbf{H}(\mathbf{k},\omega)\end{pmatrix}. \tag{2}$$

Defining $\boldsymbol{f}_n = (\mathbf{E}\ \ \mathbf{H})^{\mathrm{T}}$

$$\mathbf{M} = \begin{pmatrix}\varepsilon_0\boldsymbol{\varepsilon} & \frac{1}{c}\boldsymbol{\xi}\\ \frac{1}{c}\boldsymbol{\varsigma} & \mu_0\boldsymbol{\mu}\end{pmatrix}\ \mathbf{N} = \begin{pmatrix}0 & \mathbf{k}\times\mathbf{I}_{3\times3}\\ -\mathbf{k}\times\mathbf{I}_{3\times3} & 0\end{pmatrix} \tag{3}$$

where $\mathbf{N}$ and $\mathbf{M}$ are Hermitian (the latter since we consider lossless media), we can write Maxwell's equations as a standard eigenvalue problem

$$\mathbf{H}(\mathbf{k})\cdot\boldsymbol{f}_{n,\mathbf{k}} = \omega_{n,\mathbf{k}}\boldsymbol{f}_{n,\mathbf{k}}. \tag{4}$$

where $\mathbf{H}(\mathbf{k}) = \mathbf{M}^{-1}\cdot\mathbf{N}(\mathbf{k})$. The electromagnetic eigenfields are of the form $\tilde{\boldsymbol{f}}_n(\mathbf{r}) = \boldsymbol{f}_{n,\mathbf{k}}e^{i\mathbf{k}\cdot\mathbf{r}}$, where $\boldsymbol{f}_{n,\mathbf{k}}$ (the solution of (4)) is the envelope of the fields (independent of position). In the following, we use $\boldsymbol{f}_{n,\mathbf{k}} = \boldsymbol{f}_n(\mathbf{k})$ interchangeably.

The matrix $\mathbf{H}(\mathbf{k})$ is not itself Hermitian even through both $\mathbf{M}^{-1}$ and $\mathbf{N}$ are Hermitian, since $\mathbf{M}^{-1}$ and $\mathbf{N}$ do not commute. However, viewed as an operator, $\mathbf{H}$ is Hermitian under the inner product [51]

$$\langle\boldsymbol{f}_n|\boldsymbol{f}_m\rangle = \boldsymbol{f}_n^{\dagger}(\mathbf{k})\cdot\mathbf{M}\cdot\boldsymbol{f}_m(\mathbf{k}) \tag{5}$$

where the superscript † denotes the conjugate transpose matrix. Thus, by defining a new set of eigenvectors [6]

$$\mathbf{w}_{n,\mathbf{k}} = \mathbf{M}^{1/2}\boldsymbol{f}_{n,\mathbf{k}} \tag{6}$$

and the inner product

$$\langle\mathbf{w}_n|\mathbf{w}_m\rangle = \mathbf{w}_n^{\dagger}(\mathbf{k})\cdot\mathbf{w}_m(\mathbf{k}) \tag{7}$$

then

$$\widetilde{\mathbf{H}}(\mathbf{k})\cdot\mathbf{w}_{n,\mathbf{k}} = \omega_{n,\mathbf{k}}\mathbf{w}_{n,\mathbf{k}} \tag{8}$$

forms a Hermitian eigenvalue problem, where

$$\widetilde{\mathbf{H}}(\mathbf{k}) = \mathbf{M}^{1/2}\,\mathbf{H}(\mathbf{k})\,\mathbf{M}^{-1/2} \tag{9}$$

(that is, $\widetilde{\mathbf{H}}(\mathbf{k})$ is a Hermitian matrix). In the following, because of (6), we can work with either the eigenfunctions $\mathbf{w}_{n,\mathbf{k}}$ or $\boldsymbol{f}_{n,\mathbf{k}}$.

It is crucially important in what follows to note that (8) and the normalization condition $\langle \mathbf{w}_n | \mathbf{w}_n \rangle = 1$ define the eigenmodes only up to a phase factor.

Maxwell's equations in the form (8) is a Hermitian eigenvalue equation with eigenvalue $\omega_{n,\mathbf{k}}$ and eigenvector $\mathbf{w}_{n,\mathbf{k}}$, which contains the electric and magnetic fields, and, hence, the polarization. The matrix $\widetilde{\mathbf{H}}(\mathbf{k})$ plays the role of the Hamiltonian in quantum mechanics, i.e., it describes how the systems evolves as momentum changes. In considering the development of various Berry properties, what is important is to have an eigenproblem involving two or more related quantities (here, we have momentum and polarization). Although momentum and polarization can be put on an equal footing [22], it is usually easier to consider momentum as the parameter, and consider how polarization changes with momentum.

Briefly stated, the Berry phase is the cumulative effect of the relative phase difference between an eigenfunction at $\mathbf{k}$ and at a nearby point $\mathbf{k} + d\mathbf{k}$. Therefore, if the system changes momentum from some initial value $\mathbf{k}_i$ to some final value $\mathbf{k}_f$, the normalized eigenfunctions change correspondingly; $\mathbf{w}_n(\mathbf{k}_i) \rightarrow \mathbf{w}_n(\mathbf{k}_f)$. If the final momentum equals the initial momentum, then $\widetilde{\mathbf{H}}(\mathbf{k}_i) = \widetilde{\mathbf{H}}(\mathbf{k}_f)$, and the system environment returns to its initial value. However, the eigenfunction may not return to its initial value since eigenfunctions are defined only up to a phase factor, and for the case $\mathbf{k}_i = \mathbf{k}_f$ it may occur that $\mathbf{w}_n(\mathbf{k}_f) = e^{i\gamma_n}\mathbf{w}_n(\mathbf{k}_i)$. This anholonomy is represented by a possible additional phase factor, where γ_n is called the Berry phase. Berry phase and related quantities in a classical electromagnetics context is the topic of this paper.

A first simple example of a nontrivial Berry phase, one in which the effect is quite evident, arises from considering a curved circular waveguide supporting the dominant TE_{11} mode, as shown in Fig. 1(a) (similar to the case of the helically wound optical fiber considered in [37] and [38]. See also [52], which considered this effect before the Berry phase was understood.). As the mode propagates, it follows the waveguide, retaining the TE_{11} profile. During this evolution, the magnitude of the mode momentum, ${k_{\mathrm{TE}}}^2 = k_x^2 + k_y^2 + k_z^2$, is fixed, while its direction changes; thus, the mode traverses a path on the surface of the momentum sphere depicted in Fig. 1(b). Note, that the direction of propagation for each point of the path is normal to the sphere, and thus the electric field is necessarily tangent to the sphere. At the first bend, the direction of momentum changes from z toward x (traversing the green path on the momentum sphere), at the second bend the momentum rotates from x toward y (traversing the red path on the momentum sphere), and at the last bend the momentum changes back to its initial direction z (traversing the black path on the momentum sphere). Thus, the momentum has traversed a closed path on the momentum sphere. During this evolution, the polarization (locked to be transverse to the momentum) changes from y to x.

In this case, the change in polarization is described by a geometric phase, the Berry phase, due to parallel transport of a vector on a curved surface (a mathematical description is provided later, see also [29]). The phase determines the angle between the initial and final polarizations, and depends on the area subtended by the closed path (the phase is geometrical). Indeed, when a vector is parallel transported along a closed path, the angle between the initial and final vectors is given by the integral of the *Gaussian curvature* over the surface enclosed by the path [53]. For a sphere, this corresponds to the solid angle Ω subtended by the path. In this example, $\Omega_{\text{sphere}} = 4\pi$ and so the subtended angle is $\Omega_{\text{sphere}}/8 = \pi/2$, which represents the change from y to x polarization. Traversing a closed path along a noncurved surface does not lead to this additional angle, and so we see that a nonzero Berry phase has its origin in the curvature of momentum space (in the present case, the Gaussian curvature). Furthermore, the geometric-phase evolution of the polarization of light shown in Fig. 1 is valid when the "adiabatic approximation" holds true, i.e., the helicity (degree of circular polarization) is conserved in the evolution. Nonadiabatic corrections were discussed by Ross [52] and Berry [29].

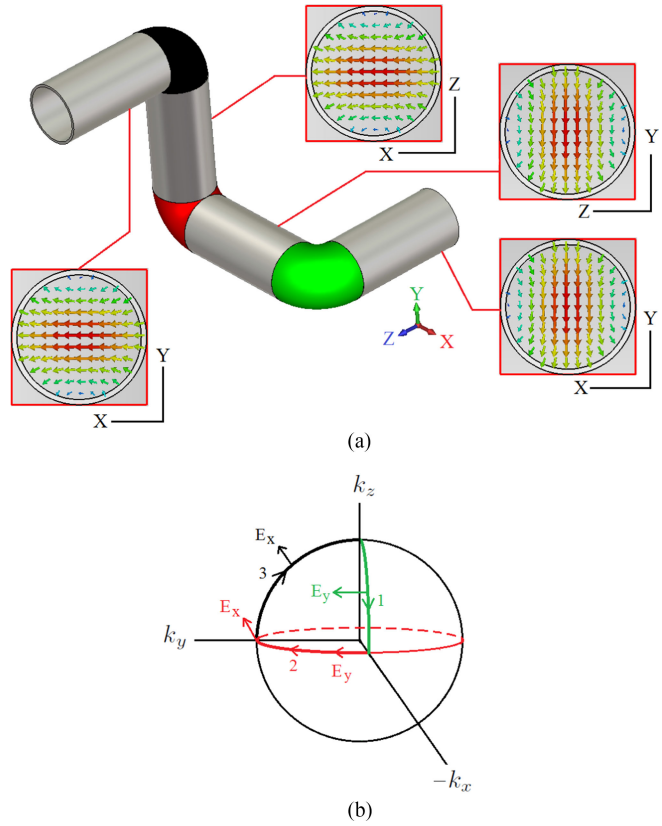

Fig. 1. (a) Curved circular waveguide demonstrating polarization rotation due to Berry phase effects and (b) momentum sphere.

Note that, for this case of transverse polarization, the polarization is normal to the momentum (i.e., we have the transversality condition $\mathbf{k} \cdot \hat{\mathbf{p}} = 0$, where $\hat{\mathbf{p}}$ is the polarization unit vector), and so at any point on the momentum sphere the polarization is always tangential to the momentum sphere, as shown in Fig. 1(b), leading to rotation of the polarization as the momentum evolves along a closed contour. If we were to consider a waveguide supporting a mode with a longitudinal component, the polarization of the longitudinal component is aligned along the direction of momentum (i.e., $\mathbf{k} \times \hat{\mathbf{p}} = 0$), and so is always normal to the momentum sphere; in this case, as the momentum evolves, this component of polarization will not incur any additional phase.

B. Berry Quantities From an Electromagnetic Perspective

In momentum ($\mathbf{k}$) space, we suppose that the eigenmode $\mathbf{w}_n(\mathbf{k})$ is initially at some point $\mathbf{k}_i$. In the quantum mechanical case one considers evolution of a system, implicitly as time progresses, during which some time-dependent parameter comes back to its initial value. Since, here, we explicitly consider time-harmonic wave phenomena, rather then system evolution, we simply consider wave propagation along some path such that the mode ends up at $\mathbf{k}_f$. If we suppose that the traversed path is closed, then $\mathbf{k}_i = \mathbf{k}_f$. Assuming well-defined and single-valued eigenmodes, we have the boundary condition $\mathbf{w}_n(\mathbf{k}_i) = e^{i\gamma_n(\mathbf{k})}\mathbf{w}_n(\mathbf{k}_f)$. At every point $\mathbf{k}$ on the path, the eigenvalue problem defines the mode up to a phase factor, which can depend on the momentum and mode index. We consider two continuous points $\mathbf{k}$ and $\mathbf{k}+d\mathbf{k}$ and corresponding eigenmodes $\mathbf{w}_n(\mathbf{k})$ and $\mathbf{w}_n(\mathbf{k}+d\mathbf{k})$. We define the differential phase $d\gamma_n$ between the two eigenmodes as [54]

$$e^{i(d\gamma_n)} = \frac{\langle \mathbf{w}_n(\mathbf{k}+d\mathbf{k})|\mathbf{w}_n(\mathbf{k})\rangle}{|\langle \mathbf{w}_n(\mathbf{k}+d\mathbf{k})|\mathbf{w}_n(\mathbf{k})\rangle|} = \frac{\mathbf{w}_n^\dagger(\mathbf{k}+d\mathbf{k})\cdot\mathbf{w}_n(\mathbf{k})}{\left|\mathbf{w}_n^\dagger(\mathbf{k}+d\mathbf{k})\cdot\mathbf{w}_n(\mathbf{k})\right|}. \tag{10}$$

The denominator is present as a normalization factor, and if the modes are already normalized, the denominator is unity since $|d\mathbf{k}| \ll |\mathbf{k}|$. The above definition is intuitive; if the eigenfunction has a $\mathbf{k}$ -dependent phase, $\mathbf{w}_n(\mathbf{k}) = e^{i\zeta(\mathbf{k})}\mathbf{g}_n(\mathbf{k})$, then $\mathbf{w}_n(\mathbf{k}+d\mathbf{k}) = e^{i\zeta(\mathbf{k}+d\mathbf{k})}\mathbf{g}_n(\mathbf{k}+d\mathbf{k})$, and so

$$\begin{aligned}\mathbf{w}_n^\dagger(\mathbf{k}+d\mathbf{k})\cdot\mathbf{w}_n(\mathbf{k}) &= e^{-i\zeta(\mathbf{k}+d\mathbf{k})}\mathbf{g}_n^*(\mathbf{k}+d\mathbf{k})\cdot e^{i\zeta(\mathbf{k})}\mathbf{g}_n(\mathbf{k}) \\ &= e^{-i\zeta(d\mathbf{k})}\left(\mathbf{g}_n^*(\mathbf{k}+d\mathbf{k})\cdot\mathbf{g}_n(\mathbf{k})\right) \\ &= e^{-i\zeta(d\mathbf{k})}\end{aligned} \tag{11}$$

assuming $\mathbf{g}_n$ are normalized in the limit $|d\mathbf{k}| \to 0$.

We expand $\mathbf{w}_n(\mathbf{k}+d\mathbf{k})$ in a Taylor series up to first order in $d\mathbf{k}$ and we expand the exponential to first order. Considering

$$\begin{aligned}\nabla_{\mathbf{k}}\langle \mathbf{w}_n|\mathbf{w}_n\rangle = \nabla_{\mathbf{k}}\mathbf{w}_n^\dagger\cdot\mathbf{w}_n + \mathbf{w}_n^\dagger\cdot\nabla_{\mathbf{k}}\mathbf{w}_n = 0 \\ \to \nabla_{\mathbf{k}}\mathbf{w}_n^\dagger\cdot\mathbf{w}_n = -\mathbf{w}_n^\dagger\cdot\nabla_{\mathbf{k}}\mathbf{w}_n\end{aligned} \tag{12}$$

we obtain

$$1 + id\gamma_n = \mathbf{w}_n^\dagger(\mathbf{k})\cdot\mathbf{w}_n(\mathbf{k}) - \mathbf{w}_n^\dagger(\mathbf{k})\cdot\nabla_{\mathbf{k}}\mathbf{w}_n(\mathbf{k})\cdot d\mathbf{k} \tag{13}$$

such that $d\gamma_n = i\mathbf{w}_n^\dagger(\mathrm{k})\cdot\nabla_{\mathrm{k}}\mathbf{w}_n(\mathrm{k})\cdot d\mathbf{k}$, and we have

$$\gamma_n = \oint_C d\mathbf{k}\cdot\mathbf{A}_n(\mathbf{k}). \tag{14}$$

The quantity

$$\mathbf{A}_n(\mathbf{k}) = i\mathbf{w}_n^\dagger(\mathbf{k})\cdot\nabla_{\mathbf{k}}\mathbf{w}_n(\mathbf{k}) = i\boldsymbol{f}_n^\dagger(\mathbf{k})\cdot\mathbf{M}\cdot\nabla_{\mathbf{k}}\boldsymbol{f}_n(\mathbf{k}) \tag{15}$$

is called the Berry connection since it connects the eigenmode $\mathbf{w}_{n,\mathbf{k}}$ at point $\mathbf{k}$ and at point $\mathbf{k}+d\mathbf{k}$; connections arise naturally in gauge theories [55]. This is also called the Berry vector potential, as an analogy to the magnetic vector potential. Because eigenmode $\mathbf{w}_n(\mathbf{k})$ is the envelope of the electromagnetic field, in calculating the Berry phase the usual electromagnetic propagator $e^{i\mathbf{k}\cdot\mathbf{r}}$ does not contribute, and the extra phase γ_n is a result of the curved geometry of momentum space.

Therefore, in addition to all other phases, the electric and magnetic fields can acquire an additional phase $e^{i\gamma_n(\mathbf{k})}$ during propagation, due to anholonomy in momentum space (from (12), it is easy to show that $\mathbf{A}_n(\mathbf{k})$ and γ_n are real-valued for real-valued $\mathbf{k}$, so that $e^{i\gamma_n(\mathbf{k})}$ is a phase, not a decay term).

1) Gauge Considerations and Real-Space Field Analogies: The electric and magnetic fields (measurable quantities) are invariant under any electromagnetic gauge transformation. The eigenvalue equation defines the eigenmodes up to a multiplicative phase factor, which is the well-known gauge ambiguity of the complex Hermitian eigenproblem. Associated with each eigenmode is a (gauge) field in momentum space, which is the Berry connection.

Multiplication of the eigenfunction $\mathbf{w}_n$ by a phase factor (a unitary transformation) represents a gauge transformation of the Berry connection; with $\mathbf{w}_n \to e^{\mathrm{i}\xi(\mathbf{k})}\mathbf{w}_n$, being $e^{\mathrm{i}\xi(\mathbf{k})}$ an arbitrary smooth unitary transformation, the Berry connection transforms to

$$\begin{aligned}\mathbf{A}_n' &= i\mathbf{w}_n^\dagger(\mathbf{k})e^{-i\xi(\mathbf{k})}\cdot\nabla_{\mathbf{k}}\left(\mathbf{w}_n(\mathbf{k})e^{i\xi(\mathbf{k})}\right) \\ &= i\mathbf{w}_n^\dagger(\mathbf{k})\cdot\nabla_{\mathbf{k}}\mathbf{w}_n(\mathbf{k}) - \nabla_{\mathbf{k}}\xi(\mathbf{k})\mathbf{w}_n^\dagger(\mathbf{k})\cdot\mathbf{w}_n(\mathbf{k}) \\ &= \mathbf{A}_n - \nabla_{\mathbf{k}}\xi(\mathbf{k})\end{aligned} \tag{16}$$

which means that the Berry connection/vector potential is gauge dependent like the electromagnetic vector potential. However, if we consider paths C that are closed in momentum space, a gauge change in (14) can only change the Berry phase by integer multiples of 2π [50]. Note that the unitary transformation $e^{\mathrm{i}\xi(\mathbf{k})}$ is required to be a smooth single-valued function of the wave vector in the vicinity of the relevant contour C, but its logarithm may not be single-valued, leading to the ambiguity of modulo 2π (gauge dependence) in the Berry phase.

Equation (14) is a momentum-space analog to the magnetic flux Φ_{mag} in terms of the real-space magnetic field and magnetic vector potential $\mathbf{A}_{\mathrm{mag}}$ in electromagnetics

$$\Phi_{\mathrm{mag}} = \int_S d\mathbf{S}\cdot\mathbf{B}(\mathbf{r}) = \oint_C d\mathbf{l}\cdot\mathbf{A}_{\mathrm{mag}}(\mathbf{r}). \tag{17}$$

A corresponding phase for a charged particle in a magnetic vector potential can be obtained upon multiplying Φ_{mag} by $e/\hbar c$ and is known as the Dirac phase. This phase was first described in [56] and underpins the Aharonov–Bohm effect [10] (the real-space analog to the Berry phase).

The real-space magnetic flux density is obtained as the curl of the vector potential

$$\mathbf{B}(\mathbf{r}) = \nabla_{\mathbf{r}}\times\mathbf{A}_{\mathrm{mag}}(\mathbf{r}) \tag{18}$$

and, similarly, a momentum-space vector field can be obtained from the curl of the Berry vector potential/Berry connection

$$\mathbf{F}_n(\mathbf{k}) = \nabla_{\mathbf{k}}\times\mathbf{A}_n(\mathbf{k}). \tag{19}$$

This field is called the Berry curvature, and can be viewed as an effective magnetic field in momentum space. In contrast to Berry connection, this field is clearly gauge independent. When the Berry connection is smoothly defined inside the surface enclosed by some contour C, it follows from Stokes' theorem that $\oint_C \mathbf{A}_n(\mathbf{k})\cdot d\mathbf{l} = \int_S \mathbf{F}_n(\mathbf{k})\cdot d\mathbf{S}$. In such a case, the Berry phase is completely determined by the Berry curvature. This

TABLE I
ANALOGY BETWEEN REAL-SPACE (EM) AND MOMENTUM-SPACE (BERRY) QUANTITIES

Real space ($\mathbf{r}$)	Momentum Space ($\mathbf{k}$)
Potential $\mathbf{A}_{\mathrm{mag}}(\mathbf{r})$	Connection $\mathbf{A}(\mathbf{k})$
Field $\mathbf{B}(\mathbf{r}) = \nabla \times \mathbf{A}_{\mathrm{mag}}(\mathbf{r})$	Curvature $\mathbf{F}(\mathbf{k}) = \nabla \times \mathbf{A}(\mathbf{k})$
Flux $\Phi_{\mathrm{mag}} = \oint_C d\mathbf{l} \cdot \mathbf{A}_{\mathrm{mag}}(\mathbf{r})$	Phase $\gamma = \oint_C d\mathbf{k} \cdot \mathbf{A}(\mathbf{k})$

result is the counterpart of that discussed earlier, where the geometric Berry phase is determined by the Gaussian curvature of the momentum space. Yet, it is important to highlight that, in general, $\mathbf{A}_n(\mathbf{k})$ may not be globally defined in all space. Moreover, in some systems it turns out that it is impossible to pick a globally defined smooth gauge of eigenfunctions (even though the whole space can be covered by different patches of smooth eigenfunctions), and it is this property that leads to the topological classification of systems as further detailed ahead.

As a partial summary, the gauge ambiguity of the Hermitian Maxwell eigenvalue problem allows for several quantities in momentum space: a geometric gauge-independent (modulo 2π) Berry phase, a gauge-dependent Berry vector potential/Berry connection (analogous to the magnetic vector potential in real space), and a gauge-independent Berry curvature (analogous to the real-space magnetic flux density). This correspondence is depicted in Table I. These quantities arise, in part, from the material medium, and in part from the type of electromagnetic mode being considered.

C. Topological Classification

From an applied electromagnetic perspective, one of the most important consequences of having nontrivial topological properties is the occurrence of one-way, back-scattering-immune surface waves at the interface between two materials with different Berry properties, specifically two materials that are topologically different. The topological classification of a system is determined by the Chern number. The Chern number is an integer obtained by integrating the Berry curvature over momentum space

$$\mathcal{C}_n = \frac{1}{2\pi} \oint_S d\mathbf{S} \cdot \mathbf{F}_n(\mathbf{k}). \tag{20}$$

In systems for which it is possible to pick a globally defined smooth gauge of eigenfunctions, and when the momentum space has no boundary (e.g., in periodic systems), it follows from Stokes' theorem that the Chern number vanishes. Hence, a nonzero Chern number indicates an obstruction to the application of Stokes' theorem to the entire momentum space. Notably, when momentum space has no boundary, the Chern number is quantized such that $\mathcal{C}_n = 0, \pm 1, \pm 2, \ldots$, is an integer. Being an integer, $\mathcal{C}_n$ must remain invariant under continuous transformations, and hence $\mathcal{C}_n$ is a topological invariant and can be used to characterize different topological phases. It is worth noting that, in general, Berry phase, connection, and curvature are geometric phenomena, while the Chern number is topological. However, the Berry phase can be topological in 2-D systems, where it is quantized and takes values of 0 or π, and in 1-D systems, where it is also known as the Zak phase [57].

The integer nature of $\mathcal{C}_n$ arises from the smoothness of the equivalent Hamiltonian and from the fact that the momentum space has no boundary. In the following, we will primarily be concerned with electromagnetic (EM) propagation in the 2-D (k_x, k_y) plane, for which the integration in (20) is over the entire 2-D wavenumber plane. Even though the 2-D (k_x, k_y) plane does not directly fit into the category of momentum spaces with no boundary, it can be transformed into a space with no boundary by including the point $\mathbf{k} = \infty$. Within this perspective, the momentum space can be mapped to the Riemann sphere, which has no boundary [41]. However, even with such a construction the equivalent Hamiltonian is generally discontinuous at $\mathbf{k} = \infty$, and, as a consequence, the Chern number cannot be guaranteed to be an integer. In practice, this problem can be fixed by introducing a spatial cutoff in the material response, as discussed in detail in [41].

In an electromagnetic continuum, it is often possible to choose the eigenfunctions globally defined and smooth in all space with exception of the point $\mathbf{k} = \infty$. In this case, taking C to be the perimeter of the infinite 2-D (k_x, k_y) plane and taking into account that the Berry phase for a contour that encloses a single point (in this case $\mathbf{k} = \infty$) is always a multiple of 2π, it follows that $1 = e^{i \oint_C d\mathbf{k} \cdot \mathbf{A}_n(\mathbf{k})} = e^{i \int_S d\mathbf{S} \cdot \mathbf{F}_n(\mathbf{k})}$ and so $\int_S d\mathbf{S} \cdot \mathbf{F}_n(\mathbf{k}) = 2\pi n$.

From an electromagnetic perspective, the Chern number can be interpreted in an intuitive way. From elementary electromagnetics, Gauss's law relates the total flux over a closed surface S to the total charge within the surface

$$\oint_S \varepsilon_0 \mathbf{E}(\mathbf{r}) \cdot d\mathbf{S} = Q^T = mq \tag{21}$$

where assuming identical charged particles, m is the number of particles and q is the charge of each particle (although often approximated as a continuum, Q^T is quantized). To keep things simple, we will assume a monopole charge of strength mq located at the origin. The electric field is given by Coulomb's law

$$\mathbf{E} = \left(\frac{mq}{4\pi\varepsilon_0} \right) \frac{\mathbf{r}}{r^3}. \tag{22}$$

The magnetic form analogous to Gauss's law

$$\oint_S \mathbf{B}(\mathbf{r}, t) \cdot d\mathbf{S} = 0 \tag{23}$$

indicates that there are no magnetic monopoles. However, if magnetic monopoles existed, the right side of (23) would be an integer mq_{mag} and the magnetic flux would be

$$\mathbf{B} = \left(\frac{mq_{\mathrm{mag}}}{4\pi} \right) \frac{\mathbf{r}}{r^3}. \tag{24}$$

In momentum space, the flux integral over a closed manifold of the Berry curvature is quantized in units of 2π, indicating the number of Berry monopoles within the surface. Berry monopoles are the momentum-space analog of a magnetic monopole, and serve as a source/sink of Berry curvature, just as the electric charge monopole mq serves as a source/sink of electric field. If the Chern number is n, the net number of Berry monopoles (whose charges do not cancel each other) is n.

The Chern number is a bulk property and is particularly important because, being an integer, it cannot be changed under continuous deformations of the system. In particular, the Chern number $\mathcal{C}_{\rm gap} = \sum_{n<n_g} \mathcal{C}_n$ associated to a subset of bands with $0 < \omega < \omega_{\rm gap}$, with $\omega_{\rm gap}$ some frequency in a complete bandgap, is unaffected by a perturbation of the material response (e.g., by a change of its structural units) unless the gap is closed. This property has remarkable consequences. Indeed, let us assume that two materials that share a common bandgap are topologically different, so that the Chern numbers associated with the bands below the gap for each material are different. This means that it is impossible to continuously transform one of the materials into the other without closing the gap. Then, if one of the materials (let us say in the region $y < 0$) is continuously transformed into the other material (let us say in region $y > \delta$) then necessarily somewhere in the transition region ($0 < y < \delta$) the bandgap must close. Thus, the transition region enables wave propagation, and because the region $y < 0$ and $y > \delta$ share a common band gap, a waveguide is formed, leading to the emergence of topologically protected edge states. It turns out that the argument is valid even in the limit $\delta \to 0$ and that the number of edge states traveling in the $+x$ and $-x$ directions are generally different. Remarkably, the difference between the Chern numbers of the two materials ($\mathcal{C}_{\rm gap,\Delta} = \mathcal{C}_2 - \mathcal{C}_1 \neq 0$) gives the difference between the number of states propagating in the two directions. This property is known as the *bulk-edge correspondence principle*. Importantly, due to the difference in the number of propagating states, it is possible to have unidirectional propagation with no backscattering in a number of physical channels that equals the Chern number difference. In the case of an electromagnetic continuum, the application of the bulk-edge correspondence requires special care, namely, it is crucial to mimic the high-frequency spatial cutoff that guarantees that the Chern numbers are integer [58].

D. Isofrequency Surfaces in Momentum Space

Let us now focus in the interesting case wherein the momentum space is a isofrequency surface, so that the relevant eigenstates are associated with the same oscillation frequency ω.

In line with a previous discussion, $\mathbf{w}_n(\mathbf{k} + d\mathbf{k})$ can always be expanded in terms of the basis $\{\mathbf{w}_m(\mathbf{k})\}_{m=1,\ldots,n,\ldots}$. In this manner, one obtains an expansion of the form $\mathbf{w}_n(\mathbf{k} + d\mathbf{k}) = \cdots + e^{-id\gamma_n}\mathbf{w}_n(\mathbf{k}) + \cdots$. (only the leading term of the expansion is shown), $d\gamma_n = \mathbf{A}_{n\mathbf{k}} \cdot d\mathbf{k}$ being the Berry phase for the path determined by $d\mathbf{k}$. Hence, the projection of $\mathbf{w}_n(\mathbf{k} + d\mathbf{k})$ onto $\mathbf{w}_n(\mathbf{k})$ is determined by the coefficient $e^{-id\gamma_n}$, consistent with (10).

Because it is assumed that the eigenstates oscillate with the same frequency in real space, it follows that the infinitesimal Berry phase $d\gamma_n$ may be regarded as a tiny time advance (or time delay). In other words, it determines if neighboring eigenstates (in the same isofrequency surface) oscillate in phase or not. When $d\gamma_n$ is nonzero the relative difference between the two neighboring eigenstates in the time domain is minimized when the eigenstates are calculated at *different* time instants, with a time advance/delay determined $d\gamma_n$. Within this perspective, the Berry curvature flux ($\nabla_{\mathbf{k}} \times \mathbf{A}_{n\mathbf{k}} \cdot \hat{\mathbf{n}} ds$) gives the accumulated Berry phase (accumulated delay, from point to point) for a small loop in the isofrequency surface with normal $\hat{n}$.

In the particular case wherein one restricts the analysis to the 2-D plane, the isofrequency surface reduces to some closed contour. The corresponding Berry phase is determined (modulo 2π) by the integral of the Berry curvature over the surface enclosed by the loop and determines the accumulated phase delay between neighboring eigenstates.

We can now revisit the first example of a curved waveguide, as shown in Fig. 1, from a mathematical perspective. Using $\mathbf{A}_{n\mathbf{k}} = i\boldsymbol{f}^{\dagger}_{n\mathbf{k}} \cdot \mathbf{M} \cdot \nabla_{\mathbf{k}} \boldsymbol{f}_{n\mathbf{k}}$, where $\mathbf{M} = \mathrm{diag}\left(\varepsilon_{0\ 3\times3}, \mu_{0\ 3\times3}\right)$ and assuming a circularly polarized (CP) field envelope

$$\mathbf{f}^{\pm}_{n\mathbf{k}} = \frac{1}{\sqrt{2\varepsilon_0}} \begin{pmatrix} \mathbf{e}_{\pm} \\ \mp\frac{1}{\eta_0} i\mathbf{e}_{\pm} \end{pmatrix} \tag{25}$$

(where $\eta_0 = \sqrt{\mu_0/\varepsilon_0}$), with $\mathbf{e}_{\pm} = \left(\widehat{\theta} \pm i\widehat{\varphi}\right)/\sqrt{2}$, then $A^{\pm}_{\mathbf{k}\theta} = i\boldsymbol{f}^{\dagger\pm}_{n\mathbf{k}} \cdot \mathbf{M} \cdot (1/k)\,\partial_{\theta} \boldsymbol{f}^{\pm}_{n\mathbf{k}} = 0$ and

$$A^{\pm}_{\mathbf{k}\varphi} = i\boldsymbol{f}^{\dagger\pm}_{n\mathbf{k}} \cdot \mathbf{M} \cdot (1/k\sin\theta)\,\partial_{\varphi} \boldsymbol{f}^{\pm}_{n\mathbf{k}} = \pm\frac{1}{k\sin\theta}\cos\theta \tag{26}$$

leading to

$$\mathbf{F}^{\pm}_{\mathbf{k}} = \mp\frac{\widehat{\mathbf{k}}}{k^2}. \tag{27}$$

Thus, we have a Berry monopole at $k = 0$, and the radial component of the Berry curvature is precisely the Gaussian curvature of the isofrequency surface. Because the accumulated phase for each CP state is symmetric (one suffers a time delay, and the other, a time advance), the linearly polarized state in Fig. 1, decomposed into two counter-propagating CP states, incurs a rotation after transversing the curved waveguide. Note that in this example, the relevant eigenspace is doubly degenerate, which is why for linear polarization the final state can be different from the initial state. For waveguides with a single mode (such as a TE_{10} mode in a rectangular waveguide), the final state is always identical to the initial state. Finally, we can note that curvature (27) together with the spherical isofrequency surface in k-space naturally yields nonzero Chern numbers for free-space light ((27) substituted into (20) leads to $C_n = \pm 2$ for the two helicity states $\pm$ [59]).

Another intuitive physical example is the following. Consider an hypothetical isotropic emitter radiating with oscillation frequency ω in an unbounded electromagnetic material. The far-field pattern is determined by the isofrequency contour of the material. For simplicity, let us suppose that the isofrequency contours are spherical surfaces. In that case, the far field in the direction $\hat{\mathbf{r}}$, it is determined by a mode with wave vector parallel to $\hat{\mathbf{r}}$. Hence, in the far-field one has $\mathbf{f} = \mathbf{f}_{\mathbf{k}} e^{i\mathbf{k}\cdot\mathbf{r}}/r$, where $\mathbf{k}$ depends on the observation direction, and $\mathbf{f}_{\mathbf{k}}$ is the envelope of a plane wave propagating along $\mathbf{k}$. Because the radiator is isotropic, the modes $\mathbf{f}_{\mathbf{k}}$ have all the same normalization (the 3-D radiation pattern intensity is independent of the observation direction). Hence, for example, the φ component of the Berry connection (tangent to the isofrequency contour) determines the differential phase delay between the emitted fields for neighboring observation directions φ and $\varphi + d\varphi$. Note that the Berry connection may depend on the considered isotropic emitter. Moreover, the relevant gauge is fixed by the emitter.

To further illustrate the idea and discuss the implications of a nontrivial Berry phase, let us consider the case where the relevant medium is air and that the isotropic emitter has a far field determined by $\mathbf{f_k} \equiv \mathbf{f}_E(\hat{\mathbf{r}})$. Note that in the present problem $\hat{\mathbf{k}}$ can be identified with $\hat{\mathbf{r}}$. Because the emitter is isotropic, one has $\langle \mathbf{f_k} | \mathbf{f_k} \rangle = \text{const.}$, independent of the observation direction.

Let us suppose that a *polarization matched* receiving antenna is placed in the far field of the emitter, let us say along the direction $\theta = \pi/2,\ \varphi = 0$. Then, the voltage induced at the open terminals of the receiver is of the form

$$\begin{aligned} V_{oc} \equiv V_{oc,0} &= -\mathbf{h}_e^R \cdot \mathbf{E}_E \\ &= -\left(h_{e,\theta}^R E_{E,\theta} + h_{e,\varphi}^R E_{E,\varphi}\right)\big|_{\varphi=0,\theta=\pi/2} \end{aligned} \quad (28)$$

where $\mathbf{h}_e^R$ is the (vector) effective length of the receiving antenna and $\mathbf{E}_E$ is the incident electric field. Since the receiving antenna is polarization matched, there is some constant A such that $\mathbf{h}_e^R = A\mathbf{E}_E^*$.

Consider that the isotropic emitter can rotate around the polar (z) axis. When the emitter is rotated by an angle $d\varphi$, the induced voltage at the terminals of the emitter is $V_{oc} = -(h_{e,\theta}^R|_{\varphi=0} E_{E,\theta}|_{\varphi=-d\varphi} + h_{e,\varphi}^R|_{\varphi=0} E_{E,\varphi}|_{\varphi=-d\varphi})$, so that for a small angle it is possible to write $V_{oc} = V_{oc,0} + \delta V_{oc}$ with

$$\delta V_{oc} = \left(h_{e,\theta}^R \partial_\varphi E_{E,\theta} + h_{e,\varphi}^R \partial_\varphi E_{E,\varphi}\right)\big|_{\varphi=0,\theta=\pi/2} d\varphi. \quad (29)$$

Taking into account that for $\theta = \pi/2,\ \varphi = 0$ one has $\partial_\varphi \hat{\theta} = 0$ and $\partial_\varphi \hat{\varphi} = -\hat{\mathbf{r}}$ one may write the induced voltage perturbation as (note that $\mathbf{h}_e^R \cdot \hat{\mathbf{r}} = 0$)

$$\delta V_{oc} = \mathbf{h}_e^R \cdot \partial_\varphi \mathbf{E}_E d\varphi. \quad (30)$$

Using the fact that the receiving antenna is polarization matched (when $d\varphi = 0$), one obtains

$$V_{oc} = V_{oc,0}\left(1 - \frac{\mathbf{E}_E^* \cdot \partial_\varphi \mathbf{E}_E}{\mathbf{E}_E^* \cdot \mathbf{E}_E} d\varphi\right). \quad (31)$$

In free-space the term in brackets can be written as a function of the six-vector $\mathbf{f}_E$ that determines the far field of the isotropic emitter: $\frac{\mathbf{E}_E^* \cdot \partial_\varphi \mathbf{E}_E}{\mathbf{E}_E^* \cdot \mathbf{E}_E} = \frac{\langle \mathbf{f}_E | \partial_\varphi \mathbf{f}_E \rangle}{\langle \mathbf{f}_E | \mathbf{f}_E \rangle}$. Hence, the induced voltage is expressed in terms of the Berry connection associated with $\mathbf{f}_E$

$$V_{oc} = V_{oc,0}\left(1 + iA_\varphi k_0 d\varphi\right). \quad (32)$$

Here, $k_0 = \omega/c$ is the free-space wavenumber and A_φ is the azimuthal component of the Berry connection. It is interesting to note that $d\gamma = -A_\varphi k_0 d\varphi$ corresponds exactly to the infinitesimal Berry phase (note that as the emitter is rotated by an angle $d\varphi$ the wave vector—from the point of view of the receiver—is effectively rotated by an angle $-d\varphi$). From here, one can write $V_{oc} \approx V_{oc,0} e^{-id\gamma}$, so that in the time domain (without loss of generality, $V_{oc,0}$ is assumed to be real-valued)

$$V_{oc}(t) \approx V_{oc,0} \cos(\omega t + d\gamma). \quad (33)$$

The physical interpretation is the following: as the isotropic emitter is rotated around the z-axis, the polarization matched receiver probes the far field in a different azimuthal direction. As neighboring states in a isofrequency contour differ approximately by a time-advance determined by the Berry phase, the induced voltage gains the phase advance $d\gamma$.

Notably, this discussion shows that a nontrivial Berry phase can have remarkable physical consequences in the considered radiation scenario. Indeed, suppose that the emitter vibrates with frequency Ω so that $d\varphi$ changes with time as $d\varphi = d\varphi_0 \cos(\Omega t)$. In such a case, the frequency spectrum of the voltage at the terminals of the matched receiver gains two spectral components due to the voltage perturbation $\delta V_{oc}(t) \approx -V_{oc,0} \sin(\omega t)\, d\gamma$. Thus, a nontrivial Berry phase leads to the appearance of two spectral lines at $\omega \pm \Omega$, reveling the analogy between the Berry phase and angular Doppler (or Coriolis) effect [59]–[65], [69]. This effect can occur only when either $E_{E,\theta}$ and/or $E_{E,\varphi}$ vary with φ in the equatorial line ($\theta = \pi/2$), for example, when the spherical field components have a φ dependence of the type $e^{in\varphi}$ with $n \neq 0$. Even though in the previous discussion the emitter was assumed to be isotropic, in practice it is enough that the radiation intensity is constant in some solid angle that contains the observation direction ($\varphi = 0$ and $\theta = \pi/2$).

Considering, e.g., $\mathbf{E}_E = E_\theta(\theta,\varphi)\,\widehat{\theta}$ where $E_\theta(\theta,\varphi) = h(\theta)\, e^{ig(\varphi)}$, then $A_\varphi = (-1/k_0)\,\partial g/\partial\varphi$. Thus, in this case, the Berry phase is proportional to the slope (Berry-phase gradient) [65] of the emitter antenna far-field phase.

E. Dispersive Material Model

For the dispersion-less material model Maxwell's equations can be written in the form of a standard Hermitian eigenvalue problem (8). However, for a dispersive lossless material model this is not the case since $\widetilde{\mathbf{H}} = \widetilde{\mathbf{H}}(\mathbf{k}, \omega)$. This nonstandard eigenvalue problem was considered in [6] for periodic materials (without magnetooptic coupling parameters), and in [41] for continuum models of dispersive lossless materials and a subclass of nonlocal materials $\mathbf{M} = \mathbf{M}(\omega, \mathbf{k}(\omega))$ including magnetooptic coupling. The details are fairly involved [41], yet the result is that defining the eigenvectors as

$$\mathbf{w}_n(\mathbf{k}) = \left[\partial_\omega\left(\omega \mathbf{M}(\omega, \mathbf{k})\right)\right]^{1/2} \cdot \boldsymbol{f}_n(\mathbf{k}) \quad (34)$$

and the inner product $\langle \mathbf{w}_n | \mathbf{w}_m \rangle = \mathbf{w}_n^\dagger \cdot \mathbf{w}_m = \boldsymbol{f}_n^\dagger(\mathbf{k}) \cdot \partial\omega\left(\omega \mathbf{M}(\omega, \mathbf{k})\right) \cdot \boldsymbol{f}_m(\mathbf{k})$ (both of which reduce to the dispersionless case, (6) and (5) for $\mathbf{M}$ a constant matrix), it is possible to define a standard Hermitian eigenvalue equation in terms of auxiliary parameters. The end result is that the formulas developed for the dispersionless case work for the dispersive case if we replace $\mathbf{M}$ with $\partial\omega(\omega\mathbf{M}(\omega, \mathbf{k}))$ in (5)–(9), leading to

$$\mathbf{A}_n(\mathbf{k}) = \mathrm{Re}\left\{ i \boldsymbol{f}_n^\dagger(\mathbf{k}) \cdot \partial\omega(\omega \mathbf{M}(\omega, \mathbf{k})) \cdot \nabla_{\mathbf{k}} \boldsymbol{f}_n(\mathbf{k}) \right\} \quad (35)$$

where the operator $\mathrm{Re}\{\cdot\}$ is unnecessary for the dispersionless case.

1) Symmetry Conditions Leading to Nontrivial Berry Connection and Curvature: In the Appendix, we show that for the lossless case, a reciprocal medium is a medium with TR symmetry and vice-versa. We also show that for TR ($\mathcal{T}$) invariant materials, $\mathbf{F}_n(\mathbf{k}) = -\mathbf{F}_n(-\mathbf{k})$, and for inversion ($\mathcal{I}$) symmetric materials, $\mathbf{F}_n(\mathbf{k}) = \mathbf{F}_n(-\mathbf{k})$.

In (20) the integral is taken over the entire plane of propagation from $\mathbf{k} \to -\infty$ to $\mathbf{k} \to +\infty$ and, therefore, Berry curvature $\mathbf{F}_n$ is comprised of both forward ($\mathbf{k} > 0$) and backward (time reversed) ($\mathbf{k} < 0$) modes. Given the odd symmetry of $\mathbf{F}_n$ for a $\mathcal{T}$-invariant material, in 2-D (e.g., the (k_x, k_y) plane) the z

component of the Berry curvature is an odd function of k_x and k_y, leading to a zero Chern number upon summing over all k values. In this case, in order to have nonzero Chern number one must break TR symmetry using, for example, a nonreciprocal material. However, as detailed in Section II-D, integration over an equifrequency surface for free-space light leads to a nonzero Chern number despite the presence of $\mathcal{T}$-invariance. Obviously, if we have both $\mathcal{T}$- and $\mathcal{I}$-symmetry for a considered mode, then $\mathbf{F}_n(\mathbf{k}) = \mathbf{0}$.

III. Example and Discussion: Magnetoplasma Materials

A prominent example of a nonreciprocal medium is obtained when we apply a magnetic field to a medium with free charges. Consider a magnetooptic medium characterized by

$$\boldsymbol{\varepsilon} = \varepsilon_0 \begin{bmatrix} \varepsilon_{11} & i\varepsilon_{12} & 0 \\ -i\varepsilon_{12} & \varepsilon_{11} & 0 \\ 0 & 0 & \varepsilon_{33} \end{bmatrix} \quad \boldsymbol{\mu} = \mu_0 \mathbf{I}_{3\times 3} \tag{36}$$

which can be realized using a plasma biased with a static magnetic field along the z direction. The elements of the permittivity tensor are dispersive

$$\varepsilon_{11} = 1 - \frac{\omega_p^2}{\omega^2 - \omega_c^2} \quad \varepsilon_{12} = \frac{-\omega_c \omega_p^2}{\omega\left(\omega^2 - \omega_c^2\right)} \quad \varepsilon_{33} = 1 - \frac{\omega_p^2}{\omega^2} \tag{37}$$

where the cyclotron frequency is $\omega_c = (q_e/m_e)\,\mathrm{B}_z$ and the plasma frequency is $\omega_p^2 = N_e q_e^2/\varepsilon_0 m_e$. In the above-mentioned equation, N_e is the free electron density, $q_e = -1.6 \times 10^{-19}$ C, and $m_e = 9.1 \times 10^{-31}$ kg are the electron charge and mass, respectively. A biased plasma has a Hermitian permittivity matrix but does not satisfy the requirements provided in the Appendix for being TR invariant.

For a biased magnetoplasma, there are two principle configurations for wave propagation, propagation along the biasing field and propagation perpendicular to the biasing field. Considering wave propagation in the bulk of a magnetoplasma medium, the associated electromagnetic waves envelopes can be obtained by finding the solution, $\boldsymbol{f}_n$, of (4), $\mathbf{H}(\mathbf{k},\omega)\cdot\boldsymbol{f}_n = \omega_n \boldsymbol{f}_n$

$$\begin{pmatrix} -\mathbf{I}_{3\times 3} & -\dfrac{\boldsymbol{\varepsilon}^{-1}}{\omega_n \varepsilon_0}\cdot\mathbf{k}\times\mathbf{I}_{3\times 3} \\ \dfrac{1}{\omega_n\mu_0}\cdot\mathbf{k}\times\mathbf{I}_{3\times 3} & -\mathbf{I}_{3\times 3} \end{pmatrix} \cdot \begin{pmatrix} \mathbf{E} \\ \mathbf{H} \end{pmatrix} = 0.$$

A. Propagation Parallel to the Static Bias

First, we suppose that the field propagates along the bias field (z -direction), which leads to the well-known Faraday rotation. From Faraday's and Ampere's law, assuming a sourceless medium, the electric field is $\mathbf{e}^{\pm} = \mathrm{E}_x^{\pm}(\hat{x} \pm i\hat{y})$, such that CP eigenfunctions are

$$\boldsymbol{f}_{nk}^{\pm} = \begin{pmatrix} \mathbf{e}^{\pm} \\ \mp i\mathrm{Y}^{\pm}\mathbf{e}^{\pm} \end{pmatrix} \tag{38}$$

where $\mathrm{k}_{\pm} = \mathrm{k}_0\sqrt{\varepsilon_{11} \mp \varepsilon_{12}}$, $\mathrm{k}_z = (\mathrm{k}_+ + \mathrm{k}_-)/2$, and $\mathrm{Y}^{\pm} = \sqrt{\varepsilon_{11} \mp \varepsilon_{12}}/\eta_0$ [66]. Based on (25)–(27), it can be seen that for a CP wave traveling along a straight path where k is constant, there is no Berry phase effect.

B. Propagation Perpendicular to the Static Bias

For the case of wave propagation perpendicular to the biasing field (no variation along z-direction, $(\partial/\partial z = 0)$), it can be shown that the modes decouple into a TE mode $(\mathrm{E}_z,\ \mathrm{H}_x,\ \mathrm{H}_y)$ and a TM mode $(\mathrm{E}_x,\ \mathrm{E}_y,\ \mathrm{H}_z)$.

For TE modes, $\mathbf{E} = \widehat{\mathbf{z}}E_z \rightarrow \mathbf{H} = \frac{\mathbf{k}}{\omega\mu_0}\times\widehat{\mathbf{z}}$ such that the eigenmodes (6×1 vectors) are

$$\boldsymbol{f}_{nk}^{\mathrm{TE}} = \begin{pmatrix} \widehat{\mathbf{z}} \\ \dfrac{\mathbf{k}}{\mu_0\omega_{nk}}\times\widehat{\mathbf{z}} \end{pmatrix} \mathrm{E}_z \tag{39}$$

and the dispersion equation is $k_x^2 + k_y^2 = \varepsilon_{33}\left(\omega_n/c\right)^2$.

For TM modes $\mathbf{H} = \hat{\mathbf{z}}\mathrm{H}_z$, $\mathbf{E} = \boldsymbol{\varepsilon}^{-1}\cdot(\hat{\mathbf{z}}\times\mathbf{k})\,/\,(\omega_n\varepsilon_0)$

$$\boldsymbol{f}_{nk}^{\mathrm{TM}} = \begin{pmatrix} \boldsymbol{\varepsilon}^{-1}\cdot\hat{\mathbf{z}}\times\dfrac{\mathbf{k}}{\varepsilon_0\omega_n} \\ \hat{\mathbf{z}} \end{pmatrix} \mathrm{H}_z \tag{40}$$

with dispersion relation

$$k_x^2 + k_y^2 = \varepsilon_{\mathrm{eff}}\left(\frac{\omega_n}{c}\right)^2 \tag{41}$$

where $\varepsilon_{\mathrm{eff}} = \left(\varepsilon_{11}^2 - \varepsilon_{12}^2\right)/\varepsilon_{11}$.

For TE modes, there is no Berry phase (in the considered gauge the eigenfunctions are real-valued, and so $\mathbf{A} = \mathbf{F} = \mathbf{0}$). For TM modes, eigenfunctions are complex-valued due to the material permittivity, allowing nontrivial Berry properties. Denoting the frequency derivative of the material response matrix, $\partial_\omega(\omega\boldsymbol{M})$ as $\beta_{11} = \partial_\omega(\omega\varepsilon_0\varepsilon_{11})$, $\beta_{12} = \partial_\omega(\omega\varepsilon_0 i\varepsilon_{12})$, it can be shown [50] that the Berry connection is

$$\mathbf{A}_n = \frac{\mathrm{Re}\{i\boldsymbol{f}_{nk}^{\dagger}\cdot\frac{1}{2}\frac{\partial}{\partial\omega}(\omega\mathbf{M}(\omega))\partial_k\boldsymbol{f}_{nk}\}}{\boldsymbol{f}_{nk}^{\dagger}\cdot\frac{1}{2}\frac{\partial}{\partial\omega}(\omega\mathbf{M}(\omega))\boldsymbol{f}_{nk}} = \frac{\mathrm{Re}\{\mathrm{N}_x\hat{\mathbf{x}} + \mathrm{N}_y\hat{\mathbf{y}}\}}{\mathrm{D}} \tag{42}$$

where

$$\begin{aligned} \mathrm{N}_x &= \tfrac{i}{(\varepsilon_0\omega_n)^2}\{-2\alpha_{11}\alpha_{12}[k_x\beta_{12} + k_y\beta_{11}] \\ &\quad +(|\alpha_{11}|^2 + |\alpha_{12}|^2)[k_x\beta_{11} - k_y\beta_{12}]\} \\ \mathrm{N}_y &= \tfrac{i}{(\varepsilon_0\omega_n)^2}\{2\alpha_{11}\alpha_{12}[k_x\beta_{11} - k_y\beta_{12}] \\ &\quad +(|\alpha_{11}|^2 + |\alpha_{12}|^2)[k_x\beta_{12} + k_y\beta_{11}]\} \\ \mathrm{D} &= \frac{|k|^2}{(\varepsilon_0\omega_n)^2}[(|\alpha_{11}|^2 + |\alpha_{12}|^2)\beta_{11} - 2\alpha_{11}\alpha_{12}\beta_{12}] + \mu_0 \end{aligned} \tag{43}$$

and

$$\alpha_{11} = \frac{\varepsilon_{11}}{\varepsilon_{11}^2 - \varepsilon_{12}^2} \quad \alpha_{12} = \frac{-i\varepsilon_{12}}{\varepsilon_{11}^2 - \varepsilon_{12}^2} \tag{44}$$

and for the Berry curvature

$$\mathbf{F}_n = \frac{\hat{\mathbf{z}}}{\mathrm{D}(\varepsilon_0\omega_n)^2}\mathrm{Re}\{i\{4\alpha_{11}\alpha_{12}\beta_{11} + 2(|\alpha_{11}|^2 + |\alpha_{12}|^2)\beta_{12}\}\}. \tag{45}$$

Fig. 2 shows the band diagram for TM modes for $\omega_p/2\pi = 10$ THz and various values of ω_c. It is clear that as $\omega_c \rightarrow 0$ (no magnetic bias, TR symmetry/reciprocity respected) the two modes become degenerate $k = 0, \omega = \omega_p$. As the bias is turned

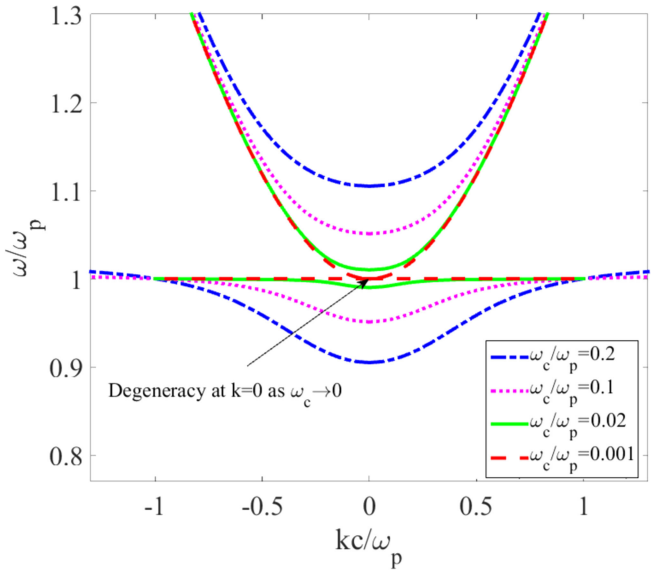

Fig. 2. Dispersion behavior of bulk TM modes for a magnetoplasma for various values of ω_c. Except for the case $\omega_c = 0$, the upper (lower) bands have Chern number +1 (-2).

on the material breaks TR symmetry $\varepsilon_{12} \neq 0$, and the two modes split apart, creating a bandgap. Note that $\nabla \cdot \mathbf{F} \neq 0$ in general, and so the "monopole" singularity discussed previously is a distributed source for this example, due to the 2-D nature of the eigenfunctions.

Details of the Chern number calculation are provided in [48] and [50], following the method presented in [41]. Using (37), the upper band has an integer Chern number, but the lower band does not. As carefully explained in [41], this is due to ill behavior of the Hamiltonian for large wavenumber. Integer Chern numbers for both branches are obtained using a nonlocal material response with a high-wavenumber spatial cutoff

$$\mathbf{M}_{\rm reg}(\omega, \mathbf{k}) = \mathbf{M}_\infty + \frac{1}{1 + \mathrm{k}^2/\mathrm{k}_{\rm max}^2} \{\mathbf{M}(\omega) - \mathbf{M}_\infty\} \quad (46)$$

where $\mathbf{M}_\infty = \lim_{\omega\to\infty} \mathbf{M}(\omega)$ and the spatial cutoff $\mathrm{k}_{\rm max}$ determines the strength of nonlocality such that as $\mathrm{k}_{\rm max} \to \infty$ the material model becomes local. For this nonlocal material response, the band diagram and Chern numbers have been obtained using $\mathrm{k}_{\rm max} = 100|\omega_c|/c$ (the Chern number calculation is insensitive to the value of $\mathrm{k}_{\rm max}$). The resulting Chern numbers for the two bands are $+1$ for the upper band and -2 for the lower band. Note that $\sum_n C_n = 0$ since there is also a mode near $\omega = 0$, not shown, that has Chern number 1 [58]. The Chern numbers are the same for all values $\omega_c > 0$. Fig. 2 was obtained using the local model, but in Fig. 5 the nonlocal dispersion behavior is shown.

In light of the distinction between the 1) spin-redirection/Rytov–Vladimirskii–Berry geometric phase and the 2) Pancharatnam–Berry phase discussed in Section I, it is worthwhile to note that the spin-redirection phase can be divided into several classes: (a) evolution along one ray as the wave propagates in an inhomogeneous medium, or a curved medium, such as the curved waveguide example of Fig. 1, and (b) relative phases between different rays (**k**-vectors) with different directions, such as considered here for the biased plasma. Other

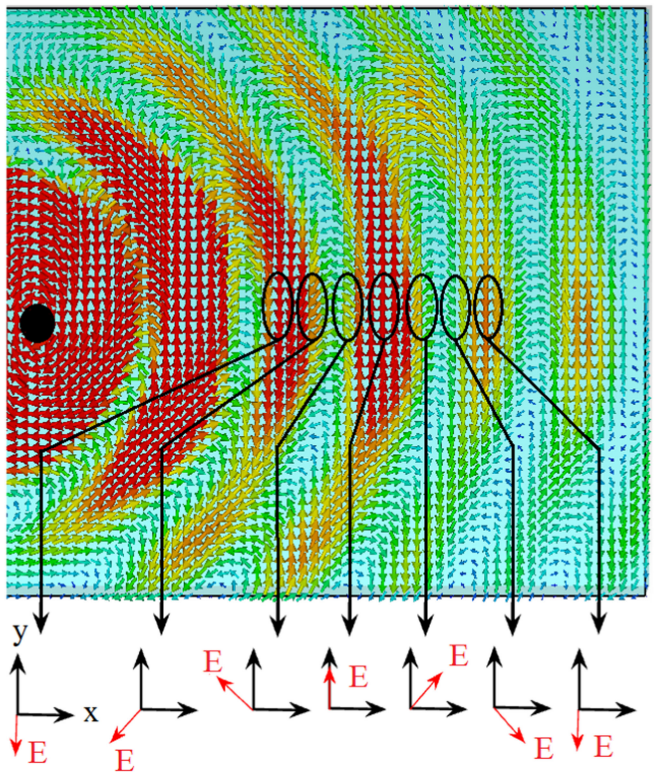

Fig. 3. Electric field radiated by a horizontal dipole (black circle) in a homogeneous plasma having $\omega/2\pi = 10$ THz, $\omega_p/\omega = 0.84$, and $\omega_c/\omega = 0.15$.

examples of case (b) are shown in [26] and [65] where the Berry phase between different rays results in the spin Hall effect and other spin-orbit phenomena.

The components of the electric field along the x and y axes in terms of H_z are

$$\mathrm{E}_x = \frac{-\varepsilon_{11}\mathrm{k}_y - i\varepsilon_{12}\mathrm{k}_x}{\varepsilon_0\omega_n(\varepsilon_{11}^2 - \varepsilon_{12}^2)}\mathrm{H}_z \quad \mathrm{E}_y = \frac{-i\varepsilon_{12}\mathrm{k}_y + \varepsilon_{11}\mathrm{k}_x}{\varepsilon_0\omega_n(\varepsilon_{11}^2 - \varepsilon_{12}^2)}\mathrm{H}_z. \quad (47)$$

Converting to a polar coordinate system (r, φ) where φ is measured from **k**

$$\mathbf{E} = E_\varphi \left(\hat{\varphi} + \hat{\mathbf{r}}\left(\frac{-i\varepsilon_{12}}{\varepsilon_{11}}\right)\right) \quad (48)$$

where $E_\varphi = kH_z/\varepsilon_0\varepsilon_{\rm eff}\omega_n$. It can be seen that there is a quadrature phase relation between the components of the electric field, which will produce a rotation of the electric field in the plane of wave propagation $(x - y)$. Generally, an elliptical polarization is produced due to nonequal ε_{11} and ε_{12}. The instantaneous electric field is

$$\mathbf{E} = \mathrm{E}_\varphi \left(\cos(\omega_n t - \mathrm{k}r)\hat{\varphi} + \frac{\varepsilon_{12}}{\varepsilon_{11}}\sin(\omega_n t - \mathrm{k}r)\hat{\mathbf{r}}\right) \quad (49)$$

where $r = \sqrt{x^2 + y^2}$. Fig. 3 shows the electric field vector due to a horizontal source in a biased magnetoplasma at a fixed instant of time, computed using CST Microwave Studio, for $\omega/2\pi = 10$ THz, $\omega_p/\omega = 0.84$, and $\omega_c/\omega = 0.15$. The ellipses span one wavelength, and highlight how the field rotates as the wave propagates (at a fixed point in space, the field also rotates as time progresses). If the bias is turned off ($\varepsilon_{12} = 0$), the material is reciprocal ($\varepsilon_{12} = 0$), the longitudinal electric field

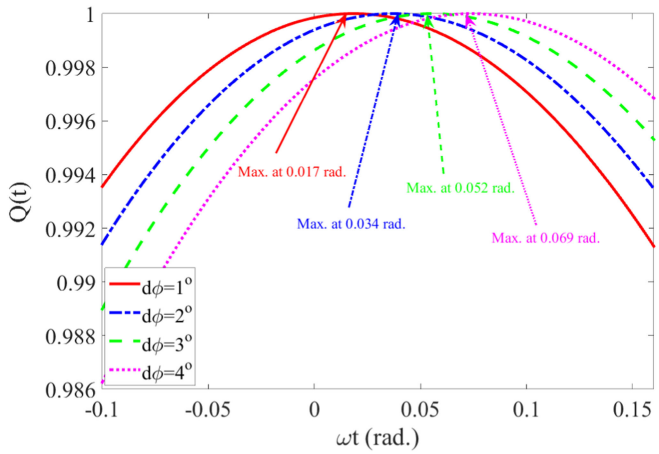

Fig. 4. $Q(t)$ versus ωt for four different momentum angles $\delta\varphi_n = n\pi/180$ radians, $n = 1, 2, 3, 4$, for $\omega/2\pi = 10$ THz, $\omega_c/2\pi = 1.73$ THz, and $\omega_p/2\pi = 9$ THz.

is zero so that the field does not rotate as described above, the eigenfunctions are real-valued, and all Berry quantities vanish ($\mathbf{A} = \mathbf{F} = \mathbf{0}$).

The Berry connection and phase are defined solely in terms of the envelope of the eigenmodes (47); the propagation factor $e^{i\mathbf{k}\cdot\mathbf{r}}$ is not involved in computing the Berry phase. As described in Section II-A, the incremental Berry phase is the relative phase difference between an eigenfunction at $\mathbf{k}$ and at a nearby point $\mathbf{k} + d\mathbf{k}$. Therefore, consistent with the operation $\nabla_{\mathbf{k}}$ used in computing $\mathbf{A}$, we consider a small change in $\mathbf{k}$ to observe the Berry phase. Since the bulk dispersion behavior is isotropic in the (k_x, k_y) plane, to change the value of $\mathbf{k}$ we need to move along an azimuthal arc at fixed radial wavenumber.

Defining the incremental Berry phase as $\delta\gamma = \mathbf{A}\cdot kd\widehat{\varphi} = A_\varphi k\delta\varphi$, and writing $\mathbf{E} = \mathbf{E}(r, \varphi, t)$, we can form a quantity

$$Q(t) = \frac{\mathbf{E}(r, 0, 0)\cdot\mathbf{E}(r, \delta\varphi, t)}{|\mathbf{E}(r, 0, 0)\cdot\mathbf{E}(r, \delta\varphi, t)|} \tag{50}$$

where r is an arbitrary fixed far-field distance, that measures the similarity between the electric field at $(t, \varphi) = (0, 0)$ and the field at $(t, \varphi) = (t, \delta\varphi)$; when the fields are the same, $Q(t) = 1$. For a given small change in $\mathbf{k}$ represented by a small change in the angle $\delta\varphi$, we expect $Q(t)$ to be maximized when $\omega t = \delta\gamma$, indicating that the incremental Berry phase $\delta\gamma$ leads to the correct time shift between nearby eigenfunctions.

As a numerical example, for $\omega/2\pi = 10$ THz, $\omega_c/2\pi = 1.73$ THz, and $\omega_p/2\pi = 9$ THz, we have bulk propagation since $\varepsilon_{\text{eff}} > 0$. We consider four small angles, $\delta\varphi_n = n\pi/180$ radians (i.e., n^{o}), $n = 1, 2, 3, 4$. For these values of $\delta\varphi_n$ the Berry phases are $\delta\gamma_1 = 0.017$ rad, $\delta\gamma_2 = 0.034$ rad, $\delta\gamma_3 = 0.052$, and $\delta\gamma_4 = 0.069$ rad, respectively. Fig. 4 indeed shows that for each angle, the Berry phase leads to the correct time shift between eigenfunctions separated by δk.

Furthermore, it should be noted that we can have Berry phase with no field rotation. For example, consider an antenna that radiates a linearly polarized plane wave that propagates along z. The antenna radiates different frequencies (in time, the fields form a traveling pulse). Assume that the amplitude of all harmonics is the same, but that the phase differs. Depending on the relative phase between harmonics, one can have a nontrivial Berry connection A_z because $\mathbf{A}$ is gauge dependent, and the relative phase (between one k value, associated with one frequency, and a nearby k value, associated with a different frequency) effectively changes the gauge. Therefore, one can have nontrivial Berry quantities in realistic physical scenarios even with linear polarizations, due to the gauge dependence (changing the phase of an eigenmode is a gauge change), and because the Berry connection along a single (nonclosed) line does not determine an invariant.

C. Edge Plasmons

SPPs are electromagnetic modes localized near the boundary between two materials, typically a material having negative permittivity and one having positive permittivity. For simple materials, these edge modes can travel in any direction along the edge. If, however, the edge mode is sufficiently nonreciprocal, it can be unidirectional. This was realized long ago for biased plasma interfaces [42]–[44]; here, we recognize the effect to be subsumed with the Berry phase/Berry curvature framework and to the topological properties of the involved materials.

The occurrence of gap Chern number $\mathcal{C}_{\text{gap},\Delta} = 1$ predicts the presence of a single, unidirectional surface mode. This can be confirmed by directly solving Maxwell's equation for surface modes at the interface of a biased plasma and a trivial medium with permittivity ε_s. Assume fields invariant along z and propagating along x, so that in the dielectric ($y > 0$) we have field variation $e^{i\mathrm{k}_{\text{spp}}x}e^{-\alpha_s y}$, and in the plasma ($y < 0$), $e^{i\mathrm{k}_{\text{spp}}x}e^{\alpha_p y}$. The condition $\alpha_p, \alpha_s > 0$ define the proper Riemann sheets for the wavenumber. Plugging into Maxwell's equations leads to the TM SPP fields

$$\begin{pmatrix} E_x \\ E_y \\ H_z \end{pmatrix} = \begin{pmatrix} E_{0x} \\ E_{0y} \\ H_{0z} \end{pmatrix} e^{i\mathrm{k}_{\text{spp}}x} \begin{cases} e^{-\alpha_s y}, & y > 0 \\ e^{\alpha_p y}, & y < 0 \end{cases} \tag{51}$$

$$E_{0x} = \frac{i\alpha_s}{\omega\varepsilon_0\varepsilon_s}H_{0z} \qquad E^s_{0y} = \frac{-\mathrm{k}_{\text{spp}}}{\omega\varepsilon_0\varepsilon_s}H_{0z} \tag{52}$$

$$E^p_{0y} = \frac{1}{\omega\varepsilon_0}\frac{\varepsilon_{12}\alpha_p - \mathrm{k}_{\text{spp}}\varepsilon_{11}}{\varepsilon^2_{11} - \varepsilon^2_{12}}H_{0z} \tag{53}$$

where $k_s^2 = \omega^2\mu\varepsilon_0\varepsilon_s$, with the SPP dispersion equation [47], [49]

$$\frac{\alpha_s}{\varepsilon_s} + \frac{\alpha_p}{\varepsilon_{\text{eff}}} = \varepsilon_{12}\frac{\mathrm{k}_{\text{spp}}}{\varepsilon_{11}\varepsilon_{\text{eff}}} \tag{54}$$

where k_{spp} is the propagation constant of the SPP along the interface, $\alpha_s = k_0\sqrt{(\mathrm{k}_{\text{spp}}/k_0)^2 - \varepsilon_s}$ and $\alpha_p = k_0\sqrt{(\mathrm{k}_{\text{spp}}/k_0)^2 - \varepsilon_{\text{eff}}}$ and $\varepsilon_{\text{eff}} = (\varepsilon^2_{11} - \varepsilon^2_{12})/\varepsilon_{11}$ are the attenuation constants in the simple and gyroelectric media, respectively. For the general case, (54) cannot be solved analytically.

1) Limit $|\varepsilon_s| \to \infty$: In the limit that $|\varepsilon_s| \to \infty$ (implementing a perfect conductor), the dispersion equation can be solved to yield $\mathrm{k}_{\text{spp}} = k_0\sqrt{\varepsilon_{11}}$, such that $\alpha_p = k_0\varepsilon_{12}/\sqrt{\varepsilon_{11}}$. For this case, $E_{0x} \to 0$ and the generally TM SPP becomes a TEM mode [42]. It is easy to see that we require $\varepsilon_{11} > 0$ to have a solution, and so we need to operate such that $\omega > \omega_p$. For $\varepsilon_{12} > 0$ there are no solutions $\mathrm{k}_{\text{spp}} < 0$, since if we take the negative root of $\sqrt{\varepsilon_{11}}$ then $\alpha_p < 0$ and the mode exponentially increases

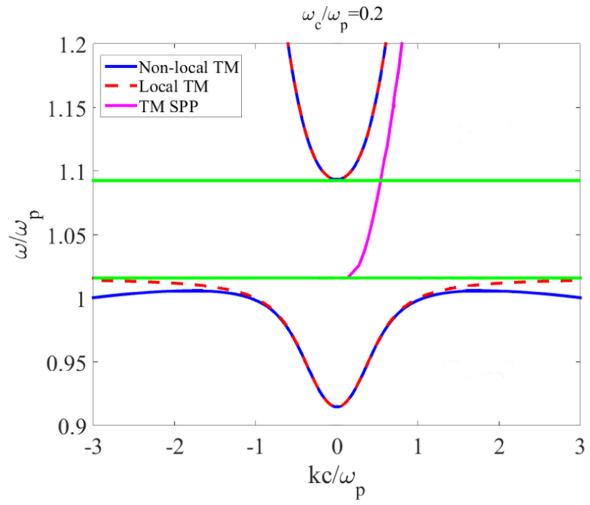

Fig. 5. Dispersion behavior of bulk (blue and dashed red) and SPP (purple) modes for the interface between perfect conductor and biased nonlocal plasma. Biased plasma has $\omega_c/\omega_p = 0.2$ and for nonlocal case $k_{\max} = 100\omega_c/c$.

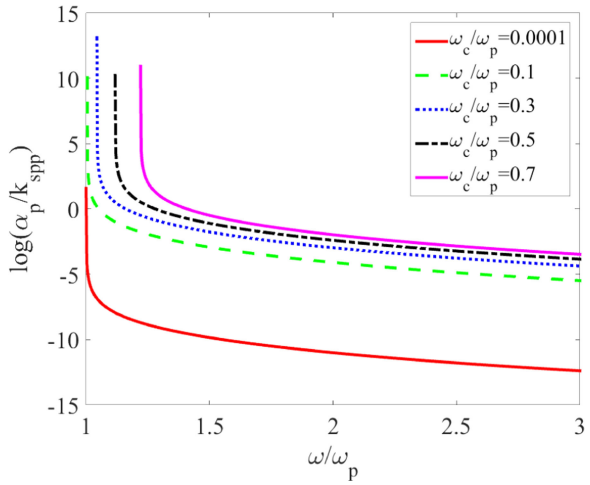

Fig. 6. Confinement factor for SPP mode for the interface between a plasma having $\omega_p/\omega = 0.97$ and a perfect conductor.

away from the interface (i.e., it is on the wrong Riemann sheet). Similarly, if we have $\varepsilon_{12} < 0$ there are no solutions $\mathrm{k_{spp}} > 0$. Therefore, we have a unidirectional SPP. For the unbiased case ($\varepsilon_{12} = 0$), there is no SPP solution.

2) $|\varepsilon_s|$ Finite: For finite values of $\varepsilon_s < 0$, an SPP is also obtained for $\omega > \omega_p$, where $\varepsilon_{11} > 0$. For $\varepsilon_s > 0$, an SPP occurs for $\omega < \omega_p$, but this case is not of interest since at a discontinuity radiation into the upper bulk region would occur.

Fig. 5 shows the bulk modes (blue and dashed red) for a biased plasma having $\omega_c/\omega_p = 0.2$, for both the local and nonlocal (46) models. Also shown is the SPP dispersion (purple) for the interface between the plasma and a perfect conductor. The SPP line crosses the gap (denoted by green lines) of the magnetoplasma with monotonic slope ($\partial_{\mathrm{k}}\omega = v_g > 0$). Fig. 6 shows the SPP confinement factor α_p as a function of frequency and bias, also for the magnetoplasma–PEC interface. As the bias is increased, the SPP becomes more confined to the interface, and as frequency increases the mode becomes less well confined. Maximum confinement occurs at $\omega = \left({\omega_p}^2 + {\omega_c}^2\right)^{1/2}$. Fig. 7

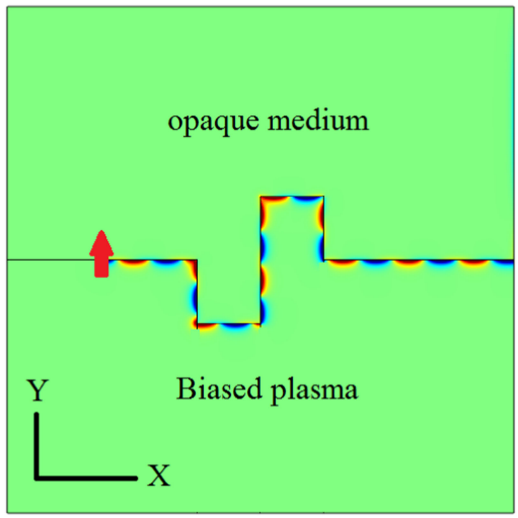

Fig. 7. SPP excited by a vertical 2-D source at the interface between a biased plasma having $\omega/2\pi = 10$ THz, $\omega_p/\omega = 0.97$, and $\omega_c/\omega = 0.173$ and an opaque material having $\varepsilon_s = -2$.

shows the electric field distribution at an interface between a biased plasma and a medium having $\varepsilon_s = -2$. Although the interface has several sharp discontinuities, since the SPP is unidirectional it cannot backscatter, and since we operate in the bandgap of the plasma, there can be no diffraction/radiation into the bulk (the $\varepsilon_s = -2$ region is opaque).

This example nicely illustrates the implications of the bulk-edge correspondence principle to topological continua. In this case, the bulk-edge correspondence works even disregarding the impact of the spatial cutoff in the waveguiding problem. In general, such effects cannot be neglected and the high-frequency cutoff needs to be mimicked in the realistic physical scenario by introducing a small air-gap in between the two materials [41], [58].

IV. Conclusion

The most celebrated property of PTIs is their capability to support one-way SPPs at an interface that are immune to backscattering from defects or imperfections. These effects were first developed at the electronic level in quantum mechanics, by systems evolving in time in a cyclic fashion. In this paper, we have demonstrated that all Berry quantities (Berry phase, connection/potential, and curvature) can be analytically obtained and interpreted from a fully classical electromagnetic perspective. We have discussed the physical meaning of the Berry phase, connection, and curvature, how these quantities arise in electromagnetic problems, and the significance of Chern numbers for unidirectional, scattering-immune SPP propagation.

Appendix

Here, we show how TR and inversion symmetry affects the Berry connection and curvature, and that for a loss-free medium, a reciprocal medium is a medium with TR symmetry and vice versa.

A. Time Reversal

TR transformation (e.g., changing $t \to -t$) for electromagnetic quantities arise from the fact that charges move in opposite directions under TR, which leaves the electric field unchanged but changes the direction of the magnetic field. Maxwell's equations are invariant under TR, and we have [67], [68]

$$\begin{aligned}\mathcal{T}\ \mathbf{E}(\mathbf{r},t) &= \mathbf{E}(\mathbf{r},-t)\,,\ \mathcal{T}\ \mathbf{D}(\mathbf{r},t) = \mathbf{D}(\mathbf{r},-t)\\ \mathcal{T}\ \mathbf{B}(\mathbf{r},t) &= -\mathbf{B}(\mathbf{r},-t)\,,\ \mathcal{T}\ \mathbf{H}(\mathbf{r},t) = -\mathbf{H}(\mathbf{r},-t)\\ \mathcal{T}\ \mathbf{J}(\mathbf{r},t) &= -\mathbf{J}(\mathbf{r},-t)\,,\ \mathcal{T}\ \rho(\mathbf{r},t) = \rho(\mathbf{r},-t)\end{aligned} \tag{55}$$

where $\mathcal{T}$ is the TR operator.

To see the effect of TR on momentum–frequency domain quantities, taking the Fourier transform of the time-reversed field $\mathbf{E}(\mathbf{r},-t)$ leads to

$$\begin{aligned}\mathcal{T}\ \mathbf{E}(\mathbf{k},\omega) &\equiv \int_{\mathbf{r}}\int_{t=-\infty}^{t=\infty} \mathcal{T}\ \mathbf{E}(\mathbf{r},t)\, e^{i\mathbf{k}\cdot\mathbf{r}} e^{-i\omega t} d\mathbf{r}dt\\ &= \int_{\mathbf{r}}\int_{t=-\infty}^{t=\infty} \mathbf{E}(\mathbf{r},-t)\, e^{i\mathbf{k}\cdot\mathbf{r}} e^{-i\omega t} d\mathbf{r}dt\\ &= -\int_{\mathbf{r}}\int_{-\tau=-\infty}^{-\tau=\infty} \mathbf{E}(\mathbf{r},\tau)\, e^{i\mathbf{k}\cdot\mathbf{r}} e^{i\omega t} d\mathbf{r}d\tau\\ &= \int_{\mathbf{r}}\int_{\tau=-\infty}^{\tau=\infty} \mathbf{E}(\mathbf{r},\tau)\, e^{i\mathbf{k}\cdot\mathbf{r}} e^{i\omega t} d\mathbf{r}d\tau\\ &= \mathbf{E}(\mathbf{k},-\omega) = \mathbf{E}^*(-\mathbf{k},\omega)\end{aligned} \tag{56}$$

where we note that applying $\mathcal{T}$ to a quantity that is not a function of time, e.g., $\mathcal{T}\mathbf{E}(\mathbf{k},\omega)$, means applying $\mathcal{T}$ in the time domain and then taking the appropriate transform. Therefore, the prescription is that applying TR in the time domain is equivalent to taking complex conjugate and reversing momentum (or, not taking complex conjugate and reversing ω). For the magnetic field, we get $\mathcal{T}\mathbf{H}(\mathbf{k},\omega) = -\mathbf{H}^*(-\mathbf{k},\omega)$.

For a source-driven problem, $\mathbf{k}$ and ω are independent parameters. However, for a source-free (eigenmode) problem, $\mathbf{k} = \mathbf{k}(\omega)$, and the momentum and frequency variables are linked by a dispersion equation (and for a trivial dispersion equation like $k = \omega\sqrt{\mu\varepsilon}$, reversing k and reversing ω are equivalent). In this case

$$\begin{aligned}\mathcal{T}\ \mathbf{E}(\mathbf{k},\omega) &\equiv \int_{\mathbf{r}}\int_{t=-\infty}^{t=\infty} \mathcal{T}\ \mathbf{E}(\mathbf{r},t)\, e^{i\mathbf{k}(\omega)\cdot\mathbf{r}} e^{-i\omega t} d\mathbf{r}dt\\ &= \int_{\mathbf{r}}\int_{t=-\infty}^{t=\infty} \mathbf{E}(\mathbf{r},-t)\, e^{i\mathbf{k}(\omega)\cdot\mathbf{r}} e^{-i\omega t} d\mathbf{r}dt\\ &= -\int_{\mathbf{r}}\int_{-\tau=-\infty}^{-\tau=\infty} \mathbf{E}(\mathbf{r},\tau)\, e^{i\mathbf{k}(\omega)\cdot\mathbf{r}} e^{i\omega\tau} d\mathbf{r}d\tau\\ &= \int_{\mathbf{r}}\int_{\tau=-\infty}^{\tau=\infty} \mathbf{E}(\mathbf{r},\tau)\, e^{i\mathbf{k}(\omega)\cdot\mathbf{r}} e^{i\omega\tau} d\mathbf{r}d\tau\\ &= \mathbf{E}^*(-\mathbf{k},\omega)\\ &= \begin{pmatrix}\mathbf{E}(\mathbf{k},-\omega) & \text{if } \mathbf{k}(\omega) = \mathbf{k}^{\text{even}}(\omega)\\ \mathbf{E}(-\mathbf{k},-\omega) & \text{if } \mathbf{k}(\omega) = \mathbf{k}^{\text{odd}}(\omega)\end{pmatrix}.\end{aligned} \tag{57}$$

Therefore,

$$\begin{aligned}\mathcal{T}\ \boldsymbol{f}_{n,\mathbf{k}(\omega)} &= \begin{pmatrix}\mathbf{E}^*(-\mathbf{k}(\omega))\\ -\mathbf{H}^*(-\mathbf{k}(\omega))\end{pmatrix} = \mathbf{T}_{6\times6}\cdot\boldsymbol{f}^*_{n,-\mathbf{k}(\omega)}\\ &= \begin{pmatrix}\mathbf{T}_{6\times6}\cdot\boldsymbol{f}_{n,\mathbf{k}(-\omega)} & \text{if } \mathbf{k}(\omega) = \mathbf{k}^{\text{even}}(\omega)\\ \mathbf{T}_{6\times6}\cdot\boldsymbol{f}_{n,-\mathbf{k}(-\omega)} & \text{if } \mathbf{k}(\omega) = \mathbf{k}^{\text{odd}}(\omega)\end{pmatrix}\end{aligned} \tag{58}$$

where

$$\mathbf{T}_{6\times6} = \begin{pmatrix}\mathbf{I}_{3\times3} & \mathbf{0}\\ 0 & -\mathbf{I}_{3\times3}\end{pmatrix} \tag{59}$$

is the Poynting vector reversing operator (applying this operator to $\boldsymbol{f}_n$ reverses the direction of the group velocity) [67], such that $\mathbf{T}_{6\times6}\cdot\mathbf{T}_{6\times6} = \mathbf{I}_{6\times6}$. Note that $\mathbf{T}_{6\times6} = \sigma_z$, the 6×6 form of the Pauli spin matrix. If the system is $\mathcal{T}$-invariant, $\mathbf{T}_{6\times6}\cdot\boldsymbol{f}^*_{n,-\mathbf{k}(\omega)} = e^{i\zeta(\mathbf{k})}\boldsymbol{f}_{n,\mathbf{k}(\omega)}$, where we can include an arbitrary phase since eigenfunctions are defined up to a phase factor. As an example, for a simple plane wave in vacuum (which is $\mathcal{T}$ -invariant), let $\mathbf{E} = \widehat{\mathbf{x}}E_0 e^{ik_0 z}$, where $k_0(\omega) = \omega\sqrt{\varepsilon_0\mu_0}$. Then, $\mathbf{H} = \widehat{\mathbf{y}}E_0(k_0/\omega\mu_0)e^{ik_0 z}$, and $\boldsymbol{f}_{n,\mathbf{k}(\omega)} = (e^{ik_0 z}, 0, 0, 0, \frac{k_0}{\omega\mu_0}e^{ik_0 z}, 0)^{\mathrm{T}}$, and it is easy to see that $\mathcal{T}\ \boldsymbol{f}_{n,\mathbf{k}(\omega)} = \mathbf{T}_{6\times6}\cdot\boldsymbol{f}^*_{n,-\mathbf{k}(\omega)} = \boldsymbol{f}_{n,\mathbf{k}(\omega)}$.

Starting with (34), we can obtain a TR eigenfunction $\mathcal{T}\ \mathbf{w}_{n,\mathbf{k}(\omega)}$ by considering that in the time domain $\mathbf{w}$ is a convolution of the inverse temporal transforms of the two terms. TR of each term leads to, by the convolution theorem, the product of the individual time-reversed temporal transforms. Using (78)

$$\begin{aligned}&\mathcal{T}\mathbf{w}_{n,\mathbf{k}(\omega)}\\ &= \mathbf{T}_{6\times6}\cdot\left[\partial_\omega\left(\omega\mathbf{M}^*(\omega,-\mathbf{k})\right)\right]^{1/2}\cdot\mathbf{T}_{6\times6}\cdot\mathbf{T}_{6\times6}\cdot\boldsymbol{f}^*_{n,-\mathbf{k}(\omega)}\\ &= \mathbf{T}_{6\times6}\cdot\mathbf{w}^*_{n,-\mathbf{k}(\omega)}.\end{aligned} \tag{60}$$

Then, it can be shown that

$$\mathcal{T}\ \mathbf{A}_n(\mathbf{k}) = \mathbf{A}_n(-\mathbf{k}) \tag{61}$$

and that, if a system is $\mathcal{T}$-invariant

$$\mathbf{A}_n(-\mathbf{k}) = \mathbf{A}_n(\mathbf{k}) + \nabla_{\mathbf{k}}\xi(\mathbf{k}) \tag{62}$$

where $\xi(\mathbf{k})$ is an arbitrary phase. To see this, consider that

$$\begin{aligned}\mathcal{T}\ \mathbf{A}_n(\mathbf{k}) &= i\left(\mathcal{T}\ \mathbf{w}_{n,\mathbf{k}}\right)^\dagger\cdot\nabla_{\mathbf{k}}\left(\mathcal{T}\ \mathbf{w}_{n,\mathbf{k}}\right)\\ &= i\ \left(\mathbf{T}_{6\times6}\cdot\mathbf{w}^*_{n,-\mathbf{k}}\right)^\dagger\cdot\nabla_{\mathbf{k}}\left(\mathbf{T}_{6\times6}\cdot\mathbf{w}^*_{n,-\mathbf{k}}\right)\\ &= i\,\mathbf{w}^{\mathrm{T}}_{n,-\mathbf{k}}\cdot\nabla_{\mathbf{k}}\mathbf{w}^*_{n,-\mathbf{k}}\\ &= -i\left(\mathbf{w}^\dagger_{n,-\mathbf{k}}\cdot\nabla_{-\mathbf{k}}\mathbf{w}_{n,-\mathbf{k}}\right) = \mathbf{A}_n(-\mathbf{k})\end{aligned} \tag{63}$$

since $\mathbf{w}^\dagger_{n,\mathbf{k}}\cdot\nabla_{\mathbf{k}}\mathbf{w}_{n,\mathbf{k}}$ is pure imaginary, proving (61). To prove (62), note that if a system is $\mathcal{T}$-invariant

$$\mathcal{T}\ \mathbf{w}_{n,\mathbf{k}}(\mathbf{k}) = e^{i\zeta(\mathbf{k})}\,\mathbf{w}_{n,\mathbf{k}} \tag{64}$$

from which (62) follows using the same arguments as in (16).

From this, for the Berry curvature

$$\begin{aligned}\mathcal{T}\,\mathbf{F}_n(\mathbf{k}) &= \nabla_{\mathbf{k}} \times (\mathcal{T}\,\mathbf{A}_n(\mathbf{k})) \\ &= \nabla_{\mathbf{k}} \times (\mathbf{A}_n(-\mathbf{k}))) \\ &= -\nabla_{-\mathbf{k}} \times (\mathbf{A}_n(-\mathbf{k}))) \\ &= -\mathbf{F}_n(-\mathbf{k}). \end{aligned} \tag{65}$$

Thus, for a system that respects TR, one can have nonzero Berry curvature, but, from (20) the Chern number will be zero ($\mathcal{T}\,\mathcal{C} = -\mathcal{C}$, such that if TR symmetry is respected, $\mathcal{C} = -\mathcal{C}$ and so $\mathcal{C} = 0$).

B. Inversion

Inversion (parity) transformation means replacing $\mathbf{r}$ with $-\mathbf{r}$. Under the inversion symmetry operator $\mathcal{I}$, [68]

$$\begin{aligned}\mathcal{I}\,\mathbf{E}(\mathbf{r},t) &= -\mathbf{E}(-\mathbf{r},t) \quad \mathcal{I}\,\mathbf{D}(\mathbf{r},t) = -\mathbf{D}(-\mathbf{r},t) \\ \mathcal{I}\,\mathbf{B}(\mathbf{r},t) &= \mathbf{B}(-\mathbf{r},t) \quad \mathcal{I}\,\mathbf{H}(\mathbf{r},t) = \mathbf{H}(-\mathbf{r},t) \\ \mathcal{I}\,\mathbf{J}(\mathbf{r},t) &= -\mathbf{J}(-\mathbf{r},t) \quad \mathcal{I}\,\rho(\mathbf{r},t) = \rho(-\mathbf{r},t) \end{aligned} \tag{66}$$

To see the effect of $\mathcal{I}$ on momentum–frequency domain quantities, taking the Fourier transform of the parity-reversed field $\mathbf{E}(-\mathbf{r},t)$ leads to

$$\begin{aligned}\mathcal{I}\,\mathbf{E}(\mathbf{k},\omega) &\equiv \int_{\mathbf{r}}\int_t \mathcal{I}\,\mathbf{E}(\mathbf{r},t)\,e^{i\mathbf{k}\cdot\mathbf{r}}e^{-i\omega t}d\mathbf{r}dt \\ &= -\int_{\mathbf{r}}\int_t \mathbf{E}(-\mathbf{r},t)\,e^{i\mathbf{k}\cdot\mathbf{r}}e^{-i\omega t}d\mathbf{r}dt \\ &= -\int_{\mathbf{x}}\int_t \mathbf{E}(\mathbf{x},\tau)\,e^{-i\mathbf{k}\cdot\mathbf{x}}e^{-i\omega t}d\mathbf{x}dt \\ &= -\mathbf{E}(-\mathbf{k},\omega) = -\mathbf{E}^*(\mathbf{k},-\omega)\,. \end{aligned} \tag{67}$$

Therefore, the prescription is that applying $\mathcal{I}$ in the space domain is equivalent to taking complex conjugate and reversing frequency (or, not taking complex conjugate and reversing momentum). For the magnetic field, we get $\mathcal{I}\,\mathbf{H}(\mathbf{k},\omega) = \mathbf{H}^*(\mathbf{k},-\omega)$. For the source-free case,

$$\begin{aligned}\mathcal{I}\,\mathbf{E}(\mathbf{k},\omega) &\equiv \int_{\mathbf{r}}\int_{t=-\infty}^{t=\infty} \mathcal{I}\,\mathbf{E}(\mathbf{r},t)\,e^{i\mathbf{k}(\omega)\cdot\mathbf{r}}e^{-i\omega t}d\mathbf{r}dt \\ &= -\int_{\mathbf{r}}\int_t \mathbf{E}(-\mathbf{r},t)\,e^{i\mathbf{k}(\omega)\cdot\mathbf{r}}e^{-i\omega t}d\mathbf{r}dt \\ &= \int_{-\mathbf{x}}\int_t \mathbf{E}(\mathbf{x},t)\,e^{-i\mathbf{k}(\omega)\cdot\mathbf{x}}e^{-i\omega t}d\mathbf{x}dt \\ &= -\mathbf{E}(-\mathbf{k}(\omega)) \\ &= -\begin{pmatrix}\mathbf{E}^*(\mathbf{k}(-\omega)) & \text{if } \mathbf{k}(\omega) = \mathbf{k}^{\text{even}}(\omega) \\ \mathbf{E}^*(-\mathbf{k}(-\omega)) & \text{if } \mathbf{k}(\omega) = \mathbf{k}^{\text{odd}}(\omega)\end{pmatrix}. \end{aligned} \tag{68}$$

Therefore,

$$\begin{aligned}\mathcal{I}\,\boldsymbol{f}_{n,\mathbf{k}(\omega)} &= \begin{pmatrix}-\mathbf{E}^*(\mathbf{k}(-\omega)) \\ \mathbf{H}^*(\mathbf{k}(-\omega))\end{pmatrix} = -\mathbf{T}_{6\times6}\cdot\boldsymbol{f}_{n,-\mathbf{k}(\omega)} \\ &= -\begin{pmatrix}\mathbf{T}_{6\times6}\cdot\boldsymbol{f}^*_{n,\mathbf{k}(-\omega)} & \text{if } \mathbf{k}(\omega) = \mathbf{k}^{\text{even}}(\omega) \\ \mathbf{T}_{6\times6}\cdot\boldsymbol{f}_{n,-\mathbf{k}(-\omega)} & \text{if } \mathbf{k}(\omega) = \mathbf{k}^{\text{odd}}(\omega).\end{pmatrix} \end{aligned} \tag{69}$$

If the system is $\mathcal{I}$-invariant, $-\mathbf{T}_{6\times6}\cdot\boldsymbol{f}_{n,-\mathbf{k}(\omega)} = e^{i\zeta(\mathbf{k})}\boldsymbol{f}_{n,\mathbf{k}(\omega)}$.

Starting with (34) the effect of $\mathcal{I}$ can be seen by considering that in the space domain $\mathbf{w}$ is a convolution of the inverse spatial transforms of the two terms. Space inversion of each term leads to, by the convolution theorem, the product of the individual transforms evaluated at $-\mathbf{k}$. Using (81),

$$\begin{aligned}\mathbf{w}_{n,\mathbf{k}(\omega)} &= \mathbf{T}_{6\times6}\cdot\left[\partial_\omega\left(\omega\mathbf{M}(\omega,-\mathbf{k})\right)\right]^{1/2}\cdot\mathbf{T}_{6\times6} \\ &\quad\cdot\left(\mathbf{T}_{6\times6}\cdot\boldsymbol{f}_{n,-\mathbf{k}(\omega)}\right) \\ &= \mathbf{T}_{6\times6}\cdot\mathbf{w}_{n,-\mathbf{k}(\omega).} \end{aligned} \tag{70}$$

The effect of inversion on the Berry connection is

$$\mathcal{I}\,\mathbf{A}_n(\mathbf{k}) = i\left(\mathcal{I}\,\mathbf{w}_{n,\mathbf{k}}\right)^\dagger\cdot\nabla_{\mathbf{k}}\left(\mathcal{I}\,\mathbf{w}_{n,\mathbf{k}}\right) \tag{71}$$

$$= i\,\left(\mathbf{T}_{6\times6}\cdot\mathbf{w}_{n,-\mathbf{k}}\right)^\dagger\cdot\nabla_{\mathbf{k}}\left(\mathbf{T}_{6\times6}\cdot\mathbf{w}_{n,-\mathbf{k}}\right) \tag{72}$$

$$= -i\mathbf{w}^\dagger_{n,-\mathbf{k}}\cdot\nabla_{-\mathbf{k}}\mathbf{w}_{n,-\mathbf{k}}$$

$$= -\mathbf{A}_n(-\mathbf{k}) \tag{73}$$

and that, if a system is $\mathcal{I}$-invariant

$$-\mathbf{A}_n(-\mathbf{k}) = \mathbf{A}_n(\mathbf{k}) + \nabla_{\mathbf{k}}\xi(\mathbf{k}). \tag{74}$$

From this, for the Berry curvature

$$\begin{aligned}\mathcal{I}\,\mathbf{F}_n(\mathbf{k}) &= \nabla_{\mathbf{k}} \times (\mathcal{I}\,\mathbf{A}_n(\mathbf{k})) \\ &= \nabla_{\mathbf{k}} \times (-\mathbf{A}_n(-\mathbf{k}))) \\ &= -\nabla_{-\mathbf{k}} \times (-\mathbf{A}_n(-\mathbf{k}))) \\ &= \mathbf{F}_n(-\mathbf{k}) \end{aligned} \tag{75}$$

and so if a system is invariant under $\mathcal{I}$

$$\mathbf{F}_n(\mathbf{k}) = \mathbf{F}_n(-\mathbf{k}).$$

For the Chern number, $\mathcal{I}\mathcal{C} = \mathcal{C}$. Obviously, if a system is invariant under both $\mathcal{T}$ and $\mathcal{I}$, $\mathbf{F}_n(\mathbf{k}) = \mathbf{0}$.

C. $\mathcal{T}$ and $\mathcal{I}$ Relations for Material Parameters and Reciprocity

1) Time Reversal: From (58), $\mathcal{T}\,\boldsymbol{f}_{n,\mathbf{k}(\omega)} = \boldsymbol{f}^{\text{TR}}_n = \mathbf{T}_{6\times6}\cdot\boldsymbol{f}^*_{n,-\mathbf{k}(\omega)}$, and so for $\boldsymbol{g}_{n,\mathbf{k}(\omega)} = [\mathbf{D}\ \ \mathbf{B}]^{\text{T}}$ we have $\boldsymbol{g}^{\text{TR}}_n = \mathbf{T}_{6\times6}\cdot\boldsymbol{g}^*_{n,-\mathbf{k}(\omega)}$. Considering $\boldsymbol{g}_{n,\mathbf{k}(\omega)} = \mathbf{M}(\omega,\mathbf{k})\cdot\boldsymbol{f}_{n,\mathbf{k}(\omega)}$, conjugating and changing the sign of momentum, and multiplying by the Poynting vector reversing operator yields

$$\begin{aligned}\mathbf{T}_{6\times6}\cdot\boldsymbol{g}^*_{n,-\mathbf{k}(\omega)} &= \mathbf{T}_{6\times6}\cdot\mathbf{M}(\omega,-\mathbf{k})^*\cdot\boldsymbol{f}^*_{n,-\mathbf{k}(\omega)} \\ &= \{\mathbf{T}_{6\times6}\cdot\mathbf{M}(\omega,-\mathbf{k})^*\cdot\mathbf{T}_{6\times6}\} \\ &\quad\cdot\mathbf{T}_{6\times6}\cdot\boldsymbol{f}^*_{n,-\mathbf{k}(\omega)} \end{aligned} \tag{76}$$

such that

$$\boldsymbol{g}^{\text{TR}}_n = \mathbf{M}^{\text{TR}}\cdot\boldsymbol{f}^{\text{TR}}_n \tag{77}$$

where

$$\mathbf{M}^{\mathrm{TR}}(\omega,\mathbf{k}) = \mathbf{T}_{6\times6}\cdot\mathbf{M}^{*}(\omega,-\mathbf{k})\cdot\mathbf{T}_{6\times6} = \begin{pmatrix} \varepsilon_0\boldsymbol{\varepsilon}^{*}(\omega,-\mathbf{k}) & -\frac{1}{c}\boldsymbol{\xi}^{*}(\omega,-\mathbf{k}) \\ -\frac{1}{c}\boldsymbol{\varsigma}^{*}(\omega,-\mathbf{k}) & \mu_0\boldsymbol{\mu}^{*}(\omega,-\mathbf{k}) \end{pmatrix} \quad (78)$$

is the time reversed material constitutive tensor. If we have $\mathbf{M}=\mathbf{M}^{\mathrm{TR}}$ then the medium is TR symmetric/invariant. Note that a lossy medium is never $\mathcal{T}$-invariant.

2) Space Inversion: For the inversion operator, from (69) $\mathcal{I}\,\boldsymbol{f}_{n,\mathbf{k}(\omega)}=\boldsymbol{f}^{\mathrm{I}}_{n}=-\mathbf{T}_{6\times6}\cdot\boldsymbol{f}_{n,-\mathbf{k}(\omega)}$, and so for $\boldsymbol{g}_{n,\mathbf{k}(\omega)}=[\mathbf{D}\ \mathbf{B}]^{\mathrm{T}}$, we have $\boldsymbol{g}^{\mathrm{I}}_{n}=-\mathbf{T}_{6\times6}\cdot\boldsymbol{g}_{n,-\mathbf{k}(\omega)}$. From $\boldsymbol{g}_{n,\mathbf{k}(\omega)}=\mathbf{M}(\omega,\mathbf{k})\cdot\boldsymbol{f}_{n,\mathbf{k}(\omega)}$, changing the sign of momentum and multiplying by $(-\mathbf{T}_{6\times6})$ results in

$$\begin{aligned} -\mathbf{T}_{6\times6}\cdot\boldsymbol{g}_{n,-\mathbf{k}(\omega)} &= -\mathbf{T}_{6\times6}\cdot\mathbf{M}(\omega,-\mathbf{k})\cdot\boldsymbol{f}_{n,-\mathbf{k}(\omega)} \\ &= \{\mathbf{T}_{6\times6}\cdot(-\mathbf{M}(\omega,-\mathbf{k}))\cdot\mathbf{T}_{6\times6}\} \\ &\quad\cdot\mathbf{T}_{6\times6}\cdot\boldsymbol{f}_{n,-\mathbf{k}(\omega)} \end{aligned} \quad (79)$$

such that

$$\boldsymbol{g}^{\mathrm{I}}_{n}=\mathbf{M}^{\mathrm{I}}\cdot\boldsymbol{f}^{\mathrm{I}}_{n} \quad (80)$$

where

$$\mathbf{M}^{\mathrm{I}}(\omega) = \mathbf{T}_{6\times6}\cdot(-\mathbf{M}(\omega,-\mathbf{k}))\cdot\mathbf{T}_{6\times6} = \begin{pmatrix} \varepsilon_0\boldsymbol{\varepsilon}(\omega,-\mathbf{k}) & -\frac{1}{c}\boldsymbol{\xi}(\omega,-\mathbf{k}) \\ -\frac{1}{c}\boldsymbol{\varsigma}(\omega,-\mathbf{k}) & \mu_0\boldsymbol{\mu}(\omega,-\mathbf{k}) \end{pmatrix} \quad (81)$$

is the space inverted material constitutive tensor. Chirality ($\boldsymbol{\xi},\boldsymbol{\xi}\neq0$), for example, breaks inversion symmetry.

3) Reciprocity: The Maxwell's equations in the frequency domain in the presence of an excitation may be written in a compact form as

$$\hat{N}\cdot\mathbf{F}=\omega\mathbf{M}\cdot\mathbf{F}+i\mathbf{j} \quad (82)$$

where $\hat{N}$ is a differential operator and $\mathbf{M}$ is the material matrix operator [41]. For spatially dispersive media the action of the material matrix on the electromagnetic fields $\mathbf{F}=(\,\mathbf{E}\ \mathbf{H}\,)^{T}$ should be understood as a spatial convolution. The six-vector $\mathbf{j}=(\,\mathbf{j}_e\ \mathbf{j}_m\,)^{T}$ is written in terms of the electric current density $\mathbf{j}_e$ and of the magnetic current density $\mathbf{j}_m$ (for the sake of generality we consider that both excitations are possible). In conventional media, the reciprocity theorem establishes that if $\mathbf{F}'$ and $\mathbf{F}''$ are the fields radiated by the localized (in space) currents $\mathbf{j}'$ and $\mathbf{j}''$, respectively, then

$$\int\mathbf{j}'\cdot\mathbf{T}_{6\times6}\cdot\mathbf{F}''-\mathbf{j}''\cdot\mathbf{T}_{6\times6}\cdot\mathbf{F}'dV=0. \quad (83)$$

In the following, we study in which conditions this result generalizes to spatially dispersive media. As a starting point, we note that Parseval's theorem establishes that the condition (83) is equivalent to $\int\mathbf{j}'_{\mathbf{k}}\cdot\mathbf{T}_{6\times6}\cdot\mathbf{F}''_{-\mathbf{k}}-\mathbf{j}''_{-\mathbf{k}}\cdot\mathbf{T}_{6\times6}\cdot\mathbf{F}'_{\mathbf{k}}d^3\mathbf{k}=0$, where $\mathbf{F}'_{\mathbf{k}}$ represents the Fourier transform of $\mathbf{F}'$, etc. The spectral domain fields satisfy $\hat{N}(\mathbf{k})\cdot\mathbf{F}_{\mathbf{k}}=\omega\mathbf{M}(\omega,\mathbf{k})\cdot\mathbf{F}_{\mathbf{k}}+i\mathbf{j}_{\mathbf{k}}$ which generalizes the formulation of Section II-A. Hence, it follows that

$$\int d^3\mathbf{k}\left\{\mathbf{F}''_{-\mathbf{k}}\cdot\mathbf{T}_{6\times6}\cdot\left[\hat{N}(\mathbf{k})-\mathbf{M}(\omega,\mathbf{k})\right]\cdot\mathbf{F}'_{\mathbf{k}}-\mathbf{F}'_{\mathbf{k}}\cdot\mathbf{T}_{6\times6}\cdot\left[\hat{N}(-\mathbf{k})-\mathbf{M}(\omega,-\mathbf{k})\right]\cdot\mathbf{F}''_{-\mathbf{k}}\right\}=0. \quad (84)$$

Since the sources are arbitrary, the above equation can be satisfied only when

$$\mathbf{T}_{6\times6}\cdot\left[\hat{N}(\mathbf{k})-\mathbf{M}(\omega,\mathbf{k})\right] = \left[\mathbf{T}_{6\times6}\cdot\left[\hat{N}(-\mathbf{k})-\mathbf{M}(\omega,-\mathbf{k})\right]\right]^{T}. \quad (85)$$

Using the explicit expression of the matrix $\hat{N}(\mathbf{k})$ [(3)] it is found after some manipulations that a material is reciprocal only when the respective material matrix satisfies

$$\mathbf{M}(\omega,\mathbf{k})=\mathbf{T}_{6\times6}\cdot\mathbf{M}^{T}(\omega,-\mathbf{k})\cdot\mathbf{T}_{6\times6}. \quad (86)$$

Comparing the requirements for TR symmetry and reciprocity, we conclude that a reciprocal material is $\mathcal{T}$-invariant, and a $\mathcal{T}$-invariant material is reciprocal, provided that

$$\mathbf{M}^{*}=\mathbf{M}^{\mathrm{T}}\rightarrow\mathbf{M}=\mathbf{M}^{\dagger} \quad (87)$$

i.e., that the material tensor is Hermitian. Since all lossless materials must have Hermitian matrix representations, in the loss-free case a reciprocal medium also has TR symmetry, and vice versa.

ACKNOWLEDGMENT

The authors would like to thank K. Bliokh for considerable help in improving the manuscript.

REFERENCES

[1] Z. Wang, Y. D. Chong, J. D. Joannopoulos, and M. Soljačić, "Reflection-free one-way edge modes in a gyromagnetic photonic crystal," *Phys. Rev. Lett.*, vol. 100, 2008, Art. no. 013905.

[2] Z. Yu, G. Veronis, Z. Wang, and S. Fan, "One-way electromagnetic waveguide formed at the interface between a plasmonic metal under a static magnetic field and a photonic crystal," *Phys. Rev. Lett.*, vol. 100, 2008, Art. no. 023902.

[3] Z. Wang, Y. Chong, J. D. Joannopoulos, and M. Soljačić, "Observation of unidirectional backscattering immune topological electromagnetic states," *Nature*, vol. 461, pp. 772–775, 2009.

[4] M. C. Rechtsman *et al.*, "Photonic floquet topological insulators," *Nature*, vol. 469, pp. 196–200, Apr. 2013.

[5] M. C. Rechtsman *et al.*, "Topological creation and destruction of edge states in photonic graphene," *Phys. Rev. Lett.*, vol. 111, 2013, Art. no. 103901.

[6] S. Raghu and F. D. M. Haldane, "Analogs of quantum-Hall-effect edge states in photonic crystals," *Phys. Rev.*, vol. 78, 2008, Art. no. 033834.

[7] F. D. M. Haldane and S. Raghu, "Possible realization of directional optical waveguides in photonic crystals with broken time-reversal symmetry," *Phys. Rev. Lett.*, vol. 100, 2008, Art. no. 013904.

[8] L. Lu, J. D. Joannopoulos, and M. Soljačić, "Topological photonics," *Nature Photon.*, vol. 8, pp. 821–829, 2014.

[9] D. Xiao, M-C Chang, and Qian Niu, "Berry phase effects on electronic properties," *Rev. Mod. Phys.*, vol. 113, 2010, Art. no. 19596.

[10] M. V. Berry, "Quantal phase factors accompanying adiabatic changes," *Proc. Roy. Soc. Lond.*A, Math. Phys. Eng. Sci., vol. 392, pp. 45–57, 1984.

[11] Y. Aharonov and J. Anandan, "Phase change during a cyclic quantum evolution," *Phys. Rev. Lett.*, vol. 58, pp. 1593–1596, 1987.

[12] D. J. Griffiths, *Introduction to Quantum Mechanics*. Englewood Cliffs, NJ, USA: Prentice-Hall, 1995.

[13] L. E. Ballentine, *Quantum Mechanics: A Modern Development*. Englewood Cliffs, NJ, USA: Prentice-Hall, 1990.

[14] S. I. Vinitskii, V. L. Derbov, V. M. Dubovik, B. L. Markovski, and Y. P. Stepanovskii, "Topological phases in quantum mechanics and polarization optics," *Sov. Phys.—Usp.*, vol. 33, pp. 403–428, 1990.
[15] R. Bhandary, "Polarization of light and topological phases," *Phys. Rep.*, vol. 281, pp. 1–64, 1997.
[16] Y. Ben-Aryeh , "Berry and Pancharatnam topological phases of atomic and optical systems," *J. Opt. B, Quantum Semiclassical Opt.*, vol. 6, pp. R1–R18, 2004.
[17] G. B. Malykin and V. I. Pozdnyakova, "Geometric phases in singlemode fiber lightguides and fiber ring interferometers," *Sov. Phys.—Usp.*, vol. 47, pp. 289–308, 2004.
[18] K. Y. Bliokh, "Geometrodynamics of polarized light: Berry phase and spin Hall effect in a gradient-index medium," *Phys. Rev. Lett.*, vol. 58, , 1987, Art. no. 1593.
[19] K. Y. Bliokh and Y. P. Bliokh, "Topological spin transport of photons: The optical Magnus effect and Berry phase," *Phys. Lett.*, vol. 333, pp. 181–186, 2004.
[20] M. Onoda, S. Murakami, and N. Nagaosa, "Hall effect of light," *Phys. Rev. Lett.*, vol. 93, 2004, Art. no. 083901.
[21] K. Y. Bliokh, A. Niv, V. Kleiner, and E. Hasman,"Geometrodynamics of spinning light," *Nature Photon.*, vol. 2, pp. 748–753, 2008.
[22] Y. Q. Cai, G. Papini, and W. R. Wood, "Berry's phase for photons and topology in Maxwell's theory," *J. Math. Phys.*, vol. 31, pp. 1942–1946, 1990.
[23] J. Segert, "Photon Berry's phase as a classical topological effect," *Phys. Rev.*, vol. 36, pp. 10–15, 1987.
[24] F. D. M. Haldane, "Path dependence of the geometric rotation of polarization in optical fibers," *Opt. Lett.*, vol. 11, pp. 730–732, 1986.
[25] S. G. Lipson, "Berry's phase in optical interferometry: A simple derivation," *Opt. Lett.*, vol. 15, pp. 154–155, 1990.
[26] K. Y. Bliokh, F. J. Rodriguez-Fortuno, F. Nori, and A. V. Zayats, "Spinorbit interactions of light," *Nature Photon.*, vol. 9, pp. 796–808, 2015.
[27] T. F. Jordan, "Direct calculation of the Berry phase for spins and helicities," *J. Math. Phys.*, vol. 28, pp. 1759–1760, 1987.
[28] I. Bialynicki-Birula and Z. Bialynicki-Birula , "Berry's phase in the relativistic theory of spinning particles," *Phys. Rev.*, vol. 35, pp. 2383–2387, 1987.
[29] M. V. Berry, "Interpreting the anholonomy of coiled light," *Nature*, vol. 326, pp. 277–278, 1987.
[30] M. Berry, "Anticipations of the Geometric phase," *Phys. Today*, vol. 43, pp. 34–40, 1990.
[31] S. Pancharatnam, "Generalized theory of interference, and its applications," *Proc. Indian. Acad. Sci.*, vol. 44, pp. 247–262, 1956.
[32] M. S. Smith, "Phase memory in W.K.B. and phase integral solutions of ionospheric propagation problems," *Proc. Roy. Soc. London. A, Math. Phys. Sci.*, vol. 346, pp. 59–79, 1975.
[33] K. G. Budden and M. S. Smith, "Phase memory and additional memory in W.K.B. solutions for wave propagation in stratified media," *Proc. R. Soc. London. Series A, Math. Phys. Sci.*, vol. 350, pp. 27–46, 1976.
[34] S. M. Rytov, "Transition from wave to geometrical optics," *Dokl. Akad. Nauk. SSSR*, vol. 18, pp. 263–266, 1938.
[35] V. V. Vladimirskii, "The rotation of polarization plane for curved light ray," *Dokl. Akad. Nauk. SSSR*, vol. 31, pp. 222–225, 1941.
[36] E. Bortolotti, "Memories and notes presented by fellows," *Atti della Reale Accademia dei Lincei, Matematiche e Naturali Ser. 6*, vol. 4, pp. 552–556, 1926.
[37] R. Y. Chiao and Y-S Wu, "Manifestations of Berry's topological phase for the photon," *Phys. Rev. Lett.*, vol. 57, pp. 933–936, 1986.
[38] A. Tomita and R. Y. Chiao, "Observation of Berry's topological phase by use of an optical Fiber," *Phys. Rev. Lett.*, vol. 57, pp. 937–940, 1986.
[39] S. A. Skirlo, L. Lu, and M. Soljačić, "Multimode one-way waveguides of large Chern numbers," *Phys. Rev. Lett.*, vol. 113, 2014, Art. no. 113904.
[40] K. Fang, Z. Yu, and S. Fan, "Microscopic theory of photonic one-way edge mode," *Phys. Rev.*, vol. 84, 2011, Art. no. 075477.
[41] M. G. Silveirinha, "Chern invariants for continuous media," *Phys. Rev.*, vol. 92, 2015, Art. no. 125153.
[42] S. R. Seshadri, "Excitation of surface waves on a perfectly conducting screen covered with anisotropic plasma," *IRE Trans. Microw. Theory. Techn.*, vol. MTT-10, pp. 573–578, Nov. 1962.
[43] A. Ishimaru, "Unidirectional waves in anisotropic media," in *Proc. Symp. Electromagn. Theory Antennas*, Copenhagen, Denmark, Jun. 1962, pp. 591–601.
[44] L. E. Zhukov and M. E. Raikh, "Chiral electromagnetic waves at the boundary of optical isomers: Quantum cotton-mouton effect," *Phys. Rev.*, vol. 61, 2000, Art. no. 12842.
[45] A. A. Zyuzin and V. A. Zyuzin, "Chiral electromagnetic waves in Weyl semimetals," *Phys. Rev.*, vol. 92, 2015, Art. no. 115310.
[46] B. Yang, M. Lawrence, W. Gao, Q. Guo, and S. Zhang. "One-way helical electromagnetic wave propagation supported by magnetized plasma," *Sci. Rep.*, vol. 6, 2016, Art. no. 21461.
[47] A. R. Davoyan and N. Engheta. "Theory of wave propagation in magnetized near-zero-epsilon metamaterials: Evidence for one-way photonic states and magnetically switched transparency and opacity," *Phys. Rev. Lett.*, vol. 111, 2013, Art no. 257401.
[48] S. A. Hassani Gangaraj, A. Nemilentsau, and G. W. Hanson, "The effects of three-dimensional defects on one-way surface plasmon propagation for photonic topological insulators comprised of continuum media," *Sci. Rep.*, vol. 6, 2016, Art. no. 30055.
[49] S. A. Hassani Gangaraj and G. W. Hanson, "Topologically protected unidirectional surface states in biased ferrites: Duality and application to directional couplers," *IEEE Antennas Wireless Propag. Lett.*, vol. 16, 2017, to be published, doi: 10.1109/LAWP.2016.2582905.
[50] G. W. Hanson, S. A. Hassani Gangaraj, and A. Nemilentsau, "Notes on photonic topological insulators and scattering-protected edge states—A brief introduction," 2016. arXiv:1602.02425.
[51] M. G. Silveirinha and S. I. Maslovski, "Exchange of momentum between moving matter induced by the zero-point fluctuations of the electromagnetic field," *Phys. Rev.*, vol. 86, 2012, Art. no. 042118.
[52] J. N. Ross, "The rotation of the polarization in low birefringence monomode optical fibres due to geometric effects," *Opt. Quantum Electron.*, vol. 16, pp. 455–461, Sep. 1984.
[53] T. Frankel, *The Geometry of Physics*, 3rd ed. Cambridge, U.K.: Cambridge Univ. Press, 2012.
[54] G. Grosso and G. P. Parravicini, *Solid State Physics*, 2nd ed. New York, NY, USA: Academic, 2014.
[55] J. W. Zwanziger, M. Koenig, and A. Pines, "Berry's phase," *Annu. Rev. Phys. Chem.*, vol. 41, pp. 601–646, 1990.
[56] P. A. M. Dirac, "Quantized singularities of the EM field," *Proc. Roy. Soc.*, vol. 133, pp. 60–72, 1931.
[57] J. Zak, "Berry's phase for energy bands in solids," *Phys. Rev. Lett.*, vol. 62,, 1989, Art. no. 2747.
[58] M. G. Silveirinha, "Bulk edge correspondence for topological photonic continua," *Phys. Rev.*, vol. 94, , 2016, Art. no. 205105.
[59] K. Y. Bliokh, D. Smirnova, and F. Nori, "Quantum spin Hall effect of light," *Science*, vol. 348, pp. 1448–1451, 2015.
[60] B. A. Garetz and S. Arnold, "Variable frequency shifting of circularly polarized laser radiation via a rotating half-wave retardation plate," *Opt. Commun.*, p. 1, 1979.
[61] B. A. Garetz, "Angular doppler effect," *J. Opt. Soc. Amer.*, p. 609, 1981.
[62] B. Mashhoon, "Neutron interferometry in a rotating frame of reference," *Phys. Rev. Lett.*, p. 2639, 1988.
[63] G. I. Opat, "The precession of a foucault pendulum viewed as a beat phenomenon of a conical pendulum subject to a coriolis force," *Amer. J. Phys.*, vol. 59, pp. 822–823, 1991.
[64] R. Simon, H. J. Kimble, and E. C. G. Sudarshan, "Evolving geometric phase and its dynamical manifestation as a frequency shift: An optical experiment," *Phys. Rev. Lett.*, vol. 61, pp. 19–22, 1988.
[65] K. Y. Bliokh, Y. Gorodetski, V. Kleiner, and E. Hasman, "Coriolis effect in optics: Unified geometric phase and spin-Hall effect," *Phys. Rev. Lett.*, vol. 101, 2008, Art. no. 030404.
[66] A. Ishimaru, *Electromagnetic Wave Propagation, Radiation, and Scattering*. Englewood Cliffs, NJ, USA: Prentice-Hall, 1991.
[67] C. Altman and K. Suchy, *Reciprocity, Spatial Mapping and Time Reversal in Electromagnetics*. Dordrecht, The Netherlands: Kluwer, 1991.
[68] T. G. Mackay and A. Lakhtakia, *Electromagnetic Anisotropy and Bianisotropy: A Field Guide*. Singapore: World Sci., 2009.
[69] F. Bretenaker and A. Le Floch , "Energy exchanges between a rotating retardation plate and a laser beam," *Phys. Rev. Lett.*, vol. 65, 1990, Art. no. 2316.

S. Ali Hassani Gangaraj (GS'15), photograph and biography not available at the time of publication.

Mário G. Silveirinha (S'99–M'03–SM'13–F'15), photograph and biography not available at the time of publication.

George W. Hanson (S'85–M'91–SM'98–F'09), photograph and biography not available at the time of publication.